A Formulation of a Phase-Independent Wave-Activity Flux for Stationary and Migratory Quasigeostrophic Eddies on a Zonally Varying Basic Flow

KOUTAROU TAKAYA

Department of Earth and Planetary Science, University of Tokyo, Tokyo, Japan

HISASHI NAKAMURA

Department of Earth and Planetary Science, University of Tokyo, and Institute for Global Change Research, Frontier Research System for Global Change, Tokyo, Japan

(Manuscript received 1 December 1998, in final form 1 August 2000)

ABSTRACT

A new formulation of an approximate conservation relation of wave-activity pseudomomentum is derived, which is applicable for either stationary or migratory quasigeostrophic (QG) eddies on a zonally varying basic flow. The authors utilize a combination of a quantity A that is proportional to wave enstrophy and another quantity $\mathcal{E}$ that is proportional to wave energy. Both A and $\mathcal{E}$ are approximately related to the wave-activity pseudomomentum. It is shown for QG eddies on a slowly varying, unforced nonzonal flow that a particular linear combination of A and $\mathcal{E}$, namely, $M \equiv (A + \mathcal{E})/2$, is independent of the wave phase, even if unaveraged, in the limit of a small-amplitude plane wave. In the same limit, a flux of M is also free from an oscillatory component on a scale of one-half wavelength even without any averaging. It is shown that M is conserved under steady, unforced, and nondissipative conditions and the flux of M is parallel to the local three-dimensional group velocity in the WKB limit. The authors' conservation relation based on a straightforward derivation is a generalization of that for stationary Rossby waves on a zonally uniform basic flow as derived by Plumb and others.

A dynamical interpretation is presented for each term of such a phase-independent flux of the authors or Plumb. Terms that consist of eddy heat and momentum fluxes are shown to represent systematic upstream transport of the mean-flow westerly momentum by a propagating wave packet, whereas other terms proportional to eddy streamfunction anomalies are shown to represent an ageostrophic flux of geopotential in the direction of the local group velocity. In such a flux, these two dynamical processes acting most strongly on the node lines and ridge/trough lines of the eddy streamfunction field, respectively, are appropriately combined to eliminate its phase dependency. The authors also derive generalized three-dimensional transformed Eulerian-mean equations with the residual circulation and eddy forcing both expressed in phase-independent forms.

The flux may not be particularly suited for evaluating the exact local budget of M, because of several assumptions imposed in the derivation. Nevertheless, these assumptions seem qualitatively valid in the assessment based on observed and simulated data. The wave-activity flux is a useful diagnostic tool for illustrating a "snapshot" of a propagating packet of stationary or migratory QG wave disturbances and thereby for inferring where the packet is emitted and absorbed, as verified in several applications to the data. It may also be useful for routine climate diagnoses in an operational center.

1. Introduction

For small-amplitude disturbances superimposed on a basic flow, wave activity satisfies a conservation law (or an approximate one in some circumstances); that is,

$$\frac{\partial A}{\partial t} + \nabla \cdot \mathbf{F} = D, \tag{1}$$

where A and $\mathbf{F}$ are the density of wave activity and its flux, respectively. The term D vanishes when the wave and basic flow are both conservative. When the disturbances are slowly modulated in the Wentzel–Kramers–Brillouin (WKB) sense—that is, weakly dissipated waves for which the group velocity $\mathbf{C}_g$ is well defined—a simple relation $\mathbf{F} = \mathbf{C}_g A$ holds and we can hence illustrate the wave packet propagation by plotting $\mathbf{F}$, even on a sheared basic flow. The divergence and convergence of $\mathbf{F}$ indicate where the wave packet is emitted

Corresponding author's address: Koutarou Takaya, Dept. of Earth and Planetary Sciences, Graduate School of Science, University of Tokyo, Sci. Bldg. 1, 7-3-1, Hongo, Bunkyo-ku, Tokyo 113-0033, Japan.
E-mail: takaya@aos.eps.s.u-tokyo.ac.jp

© 2001 American Meteorological Society

Unauthenticated | Downloaded 08/23/22 02:00 PM UTC

and decaying (or absorbed), respectively. Identifying these wave ''sources'' or ''sinks'' is important in understanding the dynamics behind various atmospheric phenomena. It is convenient for this purpose if **F** and *A* are independent of the wave phase so as to represent phase-averaged statistics. However, the unaveraged *A* and **F** inherently include an oscillatory component on a scale of one-half wavelength, because by definition they are quadratic terms in disturbance amplitude. This half-wavelength component can be removed with some sort of averaging.

In a traditional framework based on the separation of eddies from a zonally uniform basic flow, the conventional Eliassen–Palm (E–P) flux has been proven to be a powerful tool for diagnosing propagation of Rossby waves and their interactions with a zonal-mean flow on the meridional plane (e.g., Andrews and McIntyre 1976; Edmon et al. 1980; McIntyre 1982; Andrews et al. 1987). The E–P flux is a flux of wave-activity pseudomomentum on the meridional plane. Its meridional and vertical components include zonally averaged eddy momentum and temperature fluxes, respectively, which ensure the phase independency of the flux. Since the flux requires no time averaging, it can by nature represent a ''snapshot''[1] of the wave propagation on the meridional plane. However, it cannot represent the propagation in the zonal direction.

If one is interested in the evolution of a locally forced wave packet that influences local weather and climate, its zonal propagation needs to be diagnosed explicitly. Even the zonal inhomogeneities in a basic flow may need to be taken into account in representing the wave packet propagation. In the troposphere, especially in the wintertime Northern Hemisphere (NH), the mean westerlies meander in the presence of thermally and topographically forced planetary waves. This meander substantially modulates amplitudes and propagation characteristics of synoptic-scale, migratory cyclones and anticyclones, including the localization of major storm tracks (e.g., Blackmon et al. 1977; Wallace et al. 1988). Furthermore, it has been indicated that cyclogenesis along storm tracks may be caused by the ''downstream development'' of baroclinic wave packets (e.g., Chang 1993). Even the propagation of quasi-stationary disturbances with longer wavelengths is complicated by zonal asymmetries in the background westerlies (e.g., Simmons et al. 1983; Hoskins and Ambrizzi 1993; Naoe et al. 1997). Recent studies suggested that local absorption of stationary Rossby wave packets is instrumental in the formation of blocking phenomena at certain geographical locations where the background westerlies are weaker than the zonal average (e.g., Nakamura et al. 1997).

For transient, migratory eddies, time averaging is appropriate for eliminating the half-wavelength oscillatory component in *A* and **F**, which admits the zonal component in **F** that represents the zonal propagation. The extended E–P flux as formulated by Hoskins et al. (1983) and Trenberth (1986) has been widely used, since it can represent the zonal propagation of a (small-amplitude) wave packet relative to the time-mean flow. Plumb (1986, hereafter P86) defined a flux of wave-activity pseudomomentum that can delineate three-dimensional propagation (relative to the earth) of transient eddies embedded on a zonally asymmetric basic flow. The flux includes products of velocity and temperature perturbations. The phase independency is ensured for the flux of P86 and extended E–P flux by time averaging, but therefore they are not applicable to a snapshot analysis.

For stationary eddies, of course, time averaging is not equivalent to phase averaging and therefore inappropriate. Hence, for an analysis of stationary eddies or a snapshot analysis of migratory eddies, a conservation relation meant to represent three-dimensional wave propagation with a wave-activity flux that is free from any oscillatory component should be derived without any averaging. Plumb (1985, hereafter P85) was the first to derive such a conservation law for small-amplitude stationary eddies on a zonally uniform basic flow.[2] The wave-activity flux $\mathbf{F}_s$ based upon his conservation relation is phase independent but it includes no terms explicitly averaged. Therefore, it is suited for an analysis of stationary eddies. In fact, its usefulness has been demonstrated by him and others (e.g., P85; Karoly et al. 1989) in applications to large-scale stationary disturbances observed in the troposphere. Kuroda (1996) extended Plumb's formula to an axially symmetric flow on a sphere. Its generalization to finite-amplitude eddies has been achieved by Brunet and Haynes (1996). Since the flux of P85 and its generalized forms mentioned above were defined for a zonally uniform basic flow, however, the usefulness and applicability to the real atmosphere are somewhat limited, especially for the NH wintertime troposphere. Furthermore, in each of their derivations a supplementary nondivergent flux (e.g., **G** in P85) was introduced rather heuristically, in order to render the flux independent of wave phase. Yet, the physical meaning of such a supplementary flux as **G** is not totally clear, nor a physical interpretation of each term that composes such a phase-independent wave-activity flux.

In this study, we attempt to generalize $\mathbf{F}_s$ of P85 and

[1] Throughout this paper, we use the term ''snapshot'' to signify a particular phase of waves. It is used for referring not only to the status of waves at a particular moment but also to a composite or linear regression map that represents spatial distribution of typical local anomalies at a particular wave phase based on a number of realizations at different dates and/or times.

[2] In his paper a factor of ½ is missing in the formula of $\mathbf{F}_s$, which is apparently a typo.

Unauthenticated | Downloaded 08/23/22 02:00 PM UTC

its conservation law so as to be applicable to small-amplitude quasigeostrophic (QG) disturbances, either stationary or migratory, that are superimposed on a zonally varying basic flow. We derive an approximate conservation relation of the wave-activity pseudomomentum and its phase-independent flux through an approach different from and more straightforward than that of P85. Our flux will be shown to be parallel to the local three-dimensional group velocity of Rossby waves, and hence to be suited for a snapshot diagnosis of the three-dimensional propagation of wave packets of migratory and stationary eddies on a zonally varying basic flow. We argue through our derivation that phase-independent fluxes of ours and P85 may be interpreted as a superposition of two dynamical aspects of the QG wave packet propagation, though P85 did not clarify physical meanings of individual components of $\mathbf{F}_s$. Furthermore, a physical meaning of the supplementary flux $\mathbf{G}$ in P85 becomes clear through our particular approach, although such a flux does not appear explicitly in our derivation. It is also verified that our flux is indeed nearly phase-independent in applications to simulated and observed atmospheric data. Finally, we will derive formulas that present an instantaneous feedback from a propagating wave packet upon a basic flow on which it is embedded and the associated ageostrophic residual circulation as well. A summary of our results for stationary disturbances on a zonally varying basic flow has been published in Takaya and Nakamura (1997, hereafter TN97).

2. Formulation

Our approach to formulate a phase-independent wave-activity flux for QG eddies without any averaging is based on a simple idea. If a perturbation streamfunction (ψ') is proportional to the sine of the wave phase, wave enstrophy and wave energy are proportional to the sine squared and cosine squared, respectively. Then, an appropriate linear combination of these two quantities (one proportional to the wave enstrophy and the other to the wave energy) can be phase-independent even without averaging. In practice, a quantity A, enstrophy divided by the magnitude of the basic potential vorticity (PV) gradient, and another quantity $\mathcal{E}$, energy divided by the wave intrinsic phase speed, are both manipulated. The zonal mean of A has been related to "pseudomomentum" (e.g., Andrews and McIntyre 1976). The zonally averaged $\mathcal{E}$ has also been shown to represent pseudomomentum (Uryu 1974), that is, the second-order mean westerly momentum that a wave packet could add to (subtract from) the zonal-mean basic flow when emitted (absorbed). Thus, the phase-independent quantity M defined as $M \equiv (A + \mathcal{E})/2$ in this study is also related to the wave-activity pseudomomentum.

We begin with the PV (q) equation on the log-pressure coordinate with the QG scaling:

$$\frac{\partial q}{\partial t} + u\frac{\partial q}{\partial x} + v\frac{\partial q}{\partial y} = s, \tag{2}$$

where $(u, v)^{\mathrm{T}} = \mathbf{u} = (-\psi_y, \psi_x)^{\mathrm{T}}$ is the geostrophic velocity (superscript T indicates vector transpose), and s represents a nonconservative term. On a β plane, PV is defined as

$$q = f_0 + \beta y + \frac{\partial^2\psi}{\partial x^2} + \frac{\partial^2\psi}{\partial y^2} + \frac{f_0^2}{p}\frac{\partial}{\partial z}\left(\frac{p}{N^2}\frac{\partial\psi}{\partial z}\right), \tag{3}$$

where $f = f_0 + \beta y$ is the Coriolis parameter, $z = -H \ln p$ where $p =$ (pressure/1000 hPa) and H is a constant scale height, and $N^2 = (R_a p^\kappa/H)(\partial\theta/\partial z)$ is the buoyancy frequency squared where θ denotes potential temperature, R_a the gas constant of dry air, and κ is defined as R_a normalized by the specific heat of air for constant pressure.

We consider small-amplitude (order ϵ) perturbations on a steady zonally inhomogeneous basic flow $\mathbf{U} = (U, V, 0)^{\mathrm{T}}$. That is,

$$u = U(x, y, z) + u', \qquad v = V(x, y, z) + v',$$
$$\psi = \Psi(x, y, z) + \psi', \qquad q = Q(x, y, z) + q', \tag{4}$$

where the three-dimensional perturbations are denoted by primes. Then, after neglecting $O(\epsilon^2)$ terms, the linearized PV equation may be written as

$$\frac{\partial q'}{\partial t} + \mathbf{U}\cdot\nabla_H q' + \mathbf{u}'\cdot\nabla_H Q = s', \tag{5}$$

where

$$q' = \frac{\partial^2\psi'}{\partial x^2} + \frac{\partial^2\psi'}{\partial y^2} + \frac{f_0^2}{p}\frac{\partial}{\partial z}\left(\frac{p}{N^2}\frac{\partial\psi'}{\partial z}\right), \tag{6}$$

and ∇_H is the horizontal gradient operator. We now assume that the wavelike perturbations consist of relatively narrow ranges of wavenumber and frequency, so that they bear a well-defined phase speed. For such perturbations we define A and $\mathcal{E}$ as $A \equiv pq'^2/(2|\nabla_H Q|)$ and $\mathcal{E} \equiv pe/(|\mathbf{U}| - C_P)$,[3] respectively, where

$$e = \frac{1}{2}\left[\left(\frac{\partial\psi'}{\partial x}\right)^2 + \left(\frac{\partial\psi'}{\partial y}\right)^2 + \left(\frac{f_0}{N}\frac{\partial\psi'}{\partial z}\right)^2\right] \tag{7}$$

is wave energy and C_P the wave phase speed in the direction of $\mathbf{U}$. In the following, we use $\mathbf{C}_U$ as the vector that represents the phase propagation in the direction of $\mathbf{U}$; that is,

[3] The definition of a quantity $\mathcal{E}$ is somewhat similar to that of wave action $\mathcal{A} = [e]/\hat{\omega}$, where $\hat{\omega}$ denotes the intrinsic wave frequency and [ ] the zonal averaging. However, those two quantities have different physical properties from one another. For example, $\mathcal{A}$ is conserved in the exact sense even for a zonally varying basic flow, but $\mathcal{E}$ is so only for a zonally uniform basic flow. For disturbances with the zonal wavenumber k embedded on a zonally uniform basic flow, $k\mathcal{A} = -[\mathcal{E}]$ holds [see Bretherton and Garret (1968) and Andrews et al. (1987)].

Unauthenticated | Downloaded 08/23/22 02:00 PM UTC

$$\mathbf{C}_U = C_P\frac{\mathbf{U}}{|\mathbf{U}|} = \left(\frac{U}{|\mathbf{U}|}C_P, \frac{V}{|\mathbf{U}|}C_P, 0\right)^{\mathrm{T}}. \quad (8)$$

Note that C_P is equal to the zonal phase speed when $\mathbf{U}$ is purely zonal.

Since the wave-activity pseudomomentum is exactly conserved only for a zonally uniform basic flow, we will derive its approximate conservation relation for a zonally *varying* basic flow under the following two assumptions. First, we assume that a steady basic flow is nearly unforced; that is,

$$\mathbf{U}\cdot(\boldsymbol{\nabla}_H Q) \approx 0. \quad (9)$$

Then, $\mathbf{n} \equiv \boldsymbol{\nabla}_H Q/|\boldsymbol{\nabla}_H Q| \approx \gamma(-V, U, 0)^{\mathrm{T}}/|\mathbf{U}|$ holds, where $\mathbf{n}$ is the unit vector in the direction of the PV gradient and $\gamma = 1$ if the basic flow is "pseudoeastward" in the same sense as the terminology of Andrews (1984) and P86. Second, the standard WKB conditions are assumed, where the basic state varies slowly horizontally and vertically with scales much larger than the corresponding wavelengths of the perturbations. Specifically, $|\boldsymbol{\nabla}_H Q|$, $|\mathbf{U}|$, and $\mathbf{n}$ are assumed to vary slowly in space. We further assume C_P to be almost constant in the direction of $\mathbf{U}$.

There are at least two ways to derive an approximate conservation relation of M. One is a derivation by means of what may be called "local coordinate rotation." If at a particular location the X axis is taken to be in the direction of $\mathbf{U}$ and the Y axis to be perpendicular to it ($Y > 0$ for poleward in the NH), (5) can be converted onto the local X–Y coordinate system as

$$\frac{\partial q'}{\partial t} - \frac{\partial \Psi}{\partial Y}\frac{\partial q'}{\partial X} + \frac{\partial Q}{\partial Y}\frac{\partial \psi'}{\partial X} = s'. \quad (10)$$

From (10), we can readily obtain an approximate conservation relation of M on the (X, Y) coordinate under the aforementioned assumptions.[4] Then, after rotating the coordinate back, an explicit expression of the conservation relation on the latitude–longitude coordinate is obtained. See appendix A for details.

For another approach, we directly manipulate the linearized PV equation (5) on the latitude–longitude coordinate system. Although rather complicated manipulations are required, we adopt this method to specify where the aforementioned approximations and assumptions need to be used in our derivation. Multiplying (5) by $pq'/|\boldsymbol{\nabla}_H Q|$ yields the following equation of A:

$$\frac{\partial A}{\partial t} + p\left[\frac{\mathbf{U}\cdot\boldsymbol{\nabla}_H q'^2}{2|\boldsymbol{\nabla}_H Q|} + \mathbf{n}\cdot\mathbf{u}'q'\right] = D_1, \quad (11)$$

[4] Starting with (10), one can even derive an approximate conservation relation (31), simply following P85 based only on the equation of A. As shown below, however, our derivation is more straightforward without any need of incorporating such an unknown nondivergent flux as $\mathbf{G}$.

where $D_1 = ps'q'/|\boldsymbol{\nabla}_H Q|$. In the case where the basic state is zonally varying, the aforementioned WKB assumptions may lead to the following two approximate relations:

$$\begin{aligned}\frac{p}{|\boldsymbol{\nabla}_H Q|}\boldsymbol{\nabla}\cdot\left(\frac{\mathbf{U}q'^2}{2}\right) &= \frac{1}{|\boldsymbol{\nabla}_H Q|}\boldsymbol{\nabla}\cdot\left[\left(\frac{\mathbf{U}}{|\mathbf{U}|}(|\mathbf{U}| - C_P) + \frac{C_P\mathbf{U}}{|\mathbf{U}|}\right)\frac{pq'^2}{2}\right] \\ &\approx \boldsymbol{\nabla}\cdot\left[\left(\frac{\mathbf{U}}{|\mathbf{U}|}(|\mathbf{U}| - C_P) + \frac{C_P\mathbf{U}}{|\mathbf{U}|}\right)A\right] \\ &= \boldsymbol{\nabla}\cdot(\mathbf{N}^{(1)} + \mathbf{C}_U A),\end{aligned} \quad (12)$$

where $\mathbf{N}^{(1)} \equiv (\mathbf{U} - \mathbf{C}_U)A$, and

$$p\mathbf{n}\cdot\mathbf{u}'q' \approx \boldsymbol{\nabla}\cdot\mathbf{E}, \quad (13)$$

with $\mathbf{E}$ defined as

$$\mathbf{E} = \frac{p}{|\mathbf{U}|}\begin{pmatrix} U(\psi_x'^2 - e) + V\psi_x'\psi_y' \\ U\psi_x'\psi_y' + V(\psi_y'^2 - e) \\ \dfrac{f_0^2}{N^2}(U\psi_x'\psi_z' + V\psi_y'\psi_z') \end{pmatrix}, \quad (14)$$

where subscripts denote partial derivatives. Note that for a zonally uniform basic flow ($V = 0$), $\mathbf{E}$ is closely related to the extended E–P flux as defined by Trenberth (1986). Thus, (11) yields the following equation of A:

$$\frac{\partial A}{\partial t} + \boldsymbol{\nabla}\cdot(\mathbf{E} + \mathbf{C}_U A) + \boldsymbol{\nabla}\cdot\mathbf{N}^{(1)} = D_1. \quad (15)$$

In the case where the basic flow is zonally uniform ($V = 0$), none of the aforementioned assumptions are required and hence (15) leads to an exact conservation relation of A. Note that (15) becomes identical to (2.19) in P86 after rearrangement of some terms.

Next, we multiply (5) by $p\psi'/(|\mathbf{U}| - C_P)$ to yield the following equation of $\mathcal{E} \equiv pe/(|\mathbf{U}| - C_P)$:

$$\begin{aligned}&\frac{\partial \mathcal{E}}{\partial t} - p\frac{(\mathbf{k}\times\boldsymbol{\nabla}_H\psi')\cdot(\psi'\boldsymbol{\nabla}_H Q)}{|\mathbf{U}| - C_P} \\ &\quad - p\psi'\boldsymbol{\nabla}_H q'\cdot\left(\frac{\mathbf{U}}{|\mathbf{U}|} + \frac{\mathbf{C}_U}{|\mathbf{U}| - C_P}\right) \\ &\quad + \frac{1}{|\mathbf{U}| - C_P}\boldsymbol{\nabla}\cdot\mathbf{R}^{(1)} = D_2,\end{aligned} \quad (16)$$

where $D_2 = -ps'\psi'/(|\mathbf{U}| - C_P)$, $\mathbf{k}$ is an upward unit vector, and

$$\mathbf{R}^{(1)} = p\left(-\psi'\psi_{xt}', -\psi'\psi_{yt}', -\frac{f_0^2}{N^2}\psi'\psi_{zt}'\right)^{\mathrm{T}}.$$

Since C_P is almost constant in the direction of $\mathbf{U}$,

$$\frac{\mathbf{U}}{|\mathbf{U}|}\cdot\boldsymbol{\nabla}C_P = \frac{U}{|\mathbf{U}|}\frac{\partial C_P}{\partial x} + \frac{V}{|\mathbf{U}|}\frac{\partial C_P}{\partial y}\left(= \frac{\partial C_P}{\partial X}\right) \cong 0$$

Unauthenticated | Downloaded 08/23/22 02:00 PM UTC

holds, which is used to show that a particular term in (16) can be rewritten as

$$-p\psi'(\boldsymbol{\nabla}_H q')\cdot\frac{\mathbf{C}_U}{|\mathbf{U}| - C_P} \approx \boldsymbol{\nabla}\cdot(\mathbf{C}_U\mathcal{E}) + \frac{C_P}{|\mathbf{U}| - C_P}\left[\frac{U}{|\mathbf{U}|}\boldsymbol{\nabla}\cdot\mathbf{R}^{(2)} + \frac{V}{|\mathbf{U}|}\boldsymbol{\nabla}\cdot\mathbf{R}^{(3)}\right], \tag{17}$$

with

$$\mathbf{R}^{(2)} = p\left(-\psi'\psi'_{xx},\ -\psi'\psi'_{xy},\ -\frac{f_0^2}{N^2}(\psi'\psi'_{xz})\right)^{\mathrm{T}},$$

$$\mathbf{R}^{(3)} = p\left(-\psi'\psi'_{xy},\ -\psi'\psi'_{yy},\ -\frac{f_0^2}{N^2}(\psi'\psi'_{yz})\right)^{\mathrm{T}}. \tag{18}$$

Furthermore, another term in (16) yields

$$-p\frac{\mathbf{U}}{|\mathbf{U}|}\cdot(\psi'\boldsymbol{\nabla}_H q') \approx -p\phi\mathbf{n}\cdot(\mathbf{k}\times\boldsymbol{\nabla}_H q') \approx \boldsymbol{\nabla}\cdot\mathbf{H}, \tag{19}$$

where

$$\mathbf{H} = \frac{p}{|\mathbf{U}|}\begin{pmatrix} eU - U\psi'\psi'_{xx} - V\psi'\psi'_{xy} \\ eV - U\psi'\psi'_{xy} - V\psi'\psi'_{yy} \\ -\dfrac{f_0^2}{N^2}(U\psi'\psi'_{xz} + V\psi'\psi'_{yz}) \end{pmatrix}. \tag{20}$$

Also, for an unforced basic flow, the second term of the lhs of (16) yields the following approximate relation:

$$p\frac{(\mathbf{k}\times\boldsymbol{\nabla}_H\psi')\cdot(\psi'\boldsymbol{\nabla}_H Q)}{|\mathbf{U}| - C_P} \approx \boldsymbol{\nabla}\cdot\mathbf{N}^{(2)} \tag{21}$$

with

$$\mathbf{N}^{(2)} = \frac{\mathbf{k}\times\boldsymbol{\nabla}_H Q}{2(|\mathbf{U}| - C_P)}\psi'^2 = -\frac{1}{2}\frac{\mathbf{U}}{|\mathbf{U}|}\frac{|\boldsymbol{\nabla}_H Q|}{(|\mathbf{U}| - C_P)}\psi'^2. \tag{22}$$

Finally, under the approximations mentioned earlier, (16) is reduced to

$$\frac{\partial}{\partial t}\mathcal{E} + \boldsymbol{\nabla}\cdot(\mathbf{H} + \mathbf{C}_U\mathcal{E}) + \boldsymbol{\nabla}\cdot\mathbf{N}^{(2)} = D_2 + \frac{R}{|\mathbf{U}| - C_P}, \tag{23}$$

where the residual term R is given by

$$R = -\boldsymbol{\nabla}\cdot\mathbf{R}^{(1)} - \frac{C_P U}{|\mathbf{U}|}\boldsymbol{\nabla}\cdot\mathbf{R}^{(2)} - \frac{C_P V}{|\mathbf{U}|}\boldsymbol{\nabla}\cdot\mathbf{R}^{(3)}. \tag{24}$$

This term can be simplified as

$$\begin{aligned} R &= p\left(\frac{\partial e}{\partial t} + \frac{U}{|\mathbf{U}|}C_P\frac{\partial e}{\partial x} + \frac{V}{|\mathbf{U}|}C_P\frac{\partial e}{\partial y}\right) \\ &\quad + p\psi'\left(\frac{\partial q'}{\partial t} + \frac{U}{|\mathbf{U}|}C_P\frac{\partial q'}{\partial x} + \frac{V}{|\mathbf{U}|}C_P\frac{\partial q'}{\partial y}\right) \\ &= p\left[\frac{\partial e}{\partial t} + C_P\frac{\partial e}{\partial X} + \psi'\left(\frac{\partial q'}{\partial t} + C_P\frac{\partial q'}{\partial X}\right)\right]. \end{aligned} \tag{25}$$

For eddies with phase speed C_P, R vanishes in the almost plane-wave limit: that is, $R = 0$. Again, for a zonally uniform basic state, no such assumptions as above are required in deriving (23) and hence it represents an exact relation.

Now, we define a quantity M as

$$M \equiv \frac{1}{2}(A + \mathcal{E}) = \frac{p}{2}\left(\frac{q'^2}{2|\boldsymbol{\nabla}_H Q|} + \frac{e}{|\mathbf{U}| - C_P}\right). \tag{26}$$

For a perturbation in the form of a plane wave; that is, $\psi' = \psi_0\exp(z/2H)\sin(kx + ly + mz - \omega t)$, M is approximately represented as

$$M \approx \frac{|\mathbf{K}|^4\psi_0^2}{4|\boldsymbol{\nabla}_H Q|}, \tag{27}$$

where $\mathbf{K} = [k, l, (f_0N^{-1})m]^{\mathrm{T}}$ is the wavenumber vector and $H^{-1} \ll m$ is assumed. This relation is again exact for a zonally uniform basic state. We can interpret M as a generalization of small-amplitude pseudomomentum for QG eddies onto a zonally varying basic flow. Here M is phase independent in a sense that it is free from the half-wavelength component *without* any time or spatial averaging.

A conservation relation of M is obtained by combining (15) and (23):

$$\frac{\partial M}{\partial t} + \boldsymbol{\nabla}\cdot\mathbf{W} = D' - \boldsymbol{\nabla}\cdot\mathbf{N} + \frac{R}{2(|\mathbf{U}| - C_P)}, \tag{28}$$

where $D' = (D_1 + D_2)/2 \equiv D_0 s'$, $\mathbf{N} = (\mathbf{N}^{(1)} + \mathbf{N}^{(2)})/2$ and $\mathbf{W} = (\mathbf{E} + \mathbf{H})/2 + \mathbf{C}_U M$.

Before deriving an explicit expression of $\mathbf{W}$, we will show $\boldsymbol{\nabla}\cdot\mathbf{N}$ also represents nonconservative effects. Combining $\mathbf{N}^{(1)}$ with $\mathbf{N}^{(2)}$, we obtain

$$\mathbf{N} = \frac{p}{4}\frac{\mathbf{U}}{|\mathbf{U}|}\left(\frac{q'}{|\boldsymbol{\nabla}_H Q|} - \frac{\psi'}{|\mathbf{U}| - C_P}\right) \times [(|\mathbf{U}| - C_P)q' + |\boldsymbol{\nabla}_H Q|\psi']. \tag{29}$$

In the almost-plane wave limit, it follows from (10) that

$$\boldsymbol{\nabla}\cdot\mathbf{r}' \equiv \boldsymbol{\nabla}\cdot\frac{\mathbf{U}}{|\mathbf{U}|}[(|\mathbf{U}| - C_P)q' + |\boldsymbol{\nabla}_H Q|\psi'] \approx s', \tag{30}$$

with which (29) can be simplified as $\mathbf{N} = \frac{1}{2}\mathbf{r}'D_0$, where D_0 has been defined in (28). Since $|\mathbf{N}|$ is proportional to the forcing term, $\mathbf{N}$ can be regarded as another nonconservative term, which vanishes in the limit of a free plane wave (i.e., $s' = 0$) under the assumption of an unforced basic flow.

Unifying the nonconservative terms into $D_T = D' - \boldsymbol{\nabla}\cdot\mathbf{N} = (D_0\boldsymbol{\nabla}\cdot\mathbf{r}' - \mathbf{r}'\cdot\boldsymbol{\nabla}D_0)/2$, and noting that $R = 0$ for eddies with phase speed C_p in the almost plane-wave limit, we finally obtain an approximate conservation relation as

$$\frac{\partial M}{\partial t} + \boldsymbol{\nabla}\cdot\mathbf{W} = D_T. \tag{31}$$

Unauthenticated | Downloaded 08/23/22 02:00 PM UTC

Recalling $\mathbf{W} = \mathbf{W}_s + \mathbf{C}_U M$ where $\mathbf{W}_s \equiv (\mathbf{E} + \mathbf{H})/2$, we obtain an explicit expression of $\mathbf{W}$ from (14) and (20) as

$$\mathbf{W} = \frac{p}{2|\mathbf{U}|}\begin{pmatrix} U(\psi_x'^2 - \psi'\psi_{xx}') + V(\psi_x'\psi_y' - \psi'\psi_{xy}') \\ U(\psi_x'\psi_y' - \psi'\psi_{xy}') + V(\psi_y'^2 - \psi'\psi_{yy}') \\ \dfrac{f_0^2}{N^2}[U(\psi_x'\psi_z' - \psi'\psi_{xz}') + V(\psi_y'\psi_z' - \psi'\psi_{yz}')] \end{pmatrix} + \mathbf{C}_U M. \tag{32}$$

We stress again that a conservation law (31) is obtained without any averaging. We regard $\mathbf{W}$, defined in (32), as a phase-independent flux of pseudomomentum in the almost plane-wave limit, as it includes no half-wave length oscillatory components without any spatial- and/or time-averaging taken.[5] Therefore, the phase-independent flux $\mathbf{W}$ is suitable for a snapshot analysis of stationary or migratory eddies on a zonally varying basic flow, although a priori knowledge of C_P is required for migratory eddies ($C_P = 0$ prescribed for stationary eddies). Effects of the phase propagation appear only in the term $\mathbf{C}_U M$, and the rest (i.e., $\mathbf{W}_s$) is identical to the wave-activity flux for stationary eddies derived in TN97 ($\mathbf{W}$ in their notation). For a zonally uniform basic state where $V = 0$ and $U = U(y, z)$, (31) is exact in the almost plane-wave limit and $\mathbf{W}$ reduces to $\mathbf{F}_s$ of P85 when $C_P = 0$. Thus, we can interpret (31) as a generalized conservation law of phase-independent wave-activity pseudomomentum for small-amplitude QG eddies onto a zonally varying basic flow with its phase-independent flux.[6]

Through manipulations shown in appendix B, the group velocity $\mathbf{C}_g$ for free Rossby waves on an unforced, zonally varying basic flow may be expressed as

$$\mathbf{C}_g = \mathbf{C}_U + \frac{2|\boldsymbol{\nabla}_H Q|}{|\mathbf{K}|^4|\mathbf{U}|}\begin{pmatrix} k^2U + klV \\ klU + l^2V \\ \dfrac{f_0^2}{N^2}(kmU + lmV) \end{pmatrix}. \tag{33}$$

With (27) one can easily verify that $\mathbf{W} = \mathbf{C}_g M$ in the almost-plane wave limit, that is, $\mathbf{W}$ is parallel to the local three-dimensional group velocity. This group velocity property of $\mathbf{W}$ is consistent with the argument of Vanneste and Shepherd (1998), as the coefficients related to the basic state defining M and $\mathbf{W}$, specifically, $|\mathbf{U}|$, $|\boldsymbol{\nabla}_H Q|$, and N^2 (and C_P), are all varying slowly in space, which validates the WKB approach.

The conservation law (31) can readily be applied to QG eddies on a sphere with approximations as in P85 and P86. On a sphere, the geostrophic flow is represented by

$$u = -\frac{1}{a}\frac{\partial\psi}{\partial\phi}, \qquad v = \frac{1}{a\cos\phi}\frac{\partial\psi}{\partial\lambda}, \tag{34}$$

where a is the earth's radius, and (ϕ, λ) are latitude and longitude, respectively. Geostrophic streamfunction is defined as $\psi = \Phi/f$, where Φ is geopotential and f $(=2\Omega \sin\phi)$ the Coriolis parameter with the earth's rotation rate Ω. Then, QG PV is defined as

$$q = f + \frac{1}{a^2\cos^2\phi}\frac{\partial^2\psi}{\partial\lambda^2} + \frac{1}{a^2\cos\phi}\frac{\partial}{\partial\phi}\left(\cos\phi\frac{\partial\psi}{\partial\phi}\right) + \frac{f^2}{p}\frac{\partial}{\partial z}\left(\frac{p}{N^2}\frac{\partial\psi}{\partial z}\right). \tag{35}$$

After manipulations similar to those described earlier, the following conservation relation can be derived:

$$\frac{\partial}{\partial t}M + \boldsymbol{\nabla}\cdot\mathbf{W} = D_T \tag{36}$$

for the wave-activity (angular) pseudomomentum M, defined as

$$M = \frac{p}{2}\left(\frac{q'^2}{2|\boldsymbol{\nabla}_H Q|} + \frac{e}{|\mathbf{U}| - C_P}\right)\cos\phi, \tag{37}$$

with its phase-independent flux $\mathbf{W}$:

$$\mathbf{W} = \frac{p\cos\phi}{2|\mathbf{U}|}\begin{pmatrix} \dfrac{U}{a^2\cos^2\phi}\left[\left(\dfrac{\partial\psi'}{\partial\lambda}\right)^2 - \psi'\dfrac{\partial^2\psi'}{\partial\lambda^2}\right] + \dfrac{V}{a^2\cos\phi}\left[\dfrac{\partial\psi'}{\partial\lambda}\dfrac{\partial\psi'}{\partial\phi} - \psi'\dfrac{\partial^2\psi'}{\partial\lambda\partial\phi}\right] \\ \dfrac{U}{a^2\cos\phi}\left[\dfrac{\partial\psi'}{\partial\lambda}\dfrac{\partial\psi'}{\partial\phi} - \psi'\dfrac{\partial^2\psi'}{\partial\lambda\partial\phi}\right] + \dfrac{V}{a^2}\left[\left(\dfrac{\partial\psi'}{\partial\phi}\right)^2 - \psi'\dfrac{\partial^2\psi'}{\partial\phi^2}\right] \\ \dfrac{f_0^2}{N^2}\left\{\dfrac{U}{a\cos\phi}\left[\dfrac{\partial\psi'}{\partial\lambda}\dfrac{\partial\psi'}{\partial z} - \psi'\dfrac{\partial^2\psi'}{\partial\lambda\partial z}\right] + \dfrac{V}{a}\left[\dfrac{\partial\psi'}{\partial\phi}\dfrac{\partial\psi'}{\partial z} - \psi'\dfrac{\partial^2\psi'}{\partial\phi\partial z}\right]\right\} \end{pmatrix} + \mathbf{C}_U M, \tag{38}$$

[5] Additionally, a nonconservative term $D_T = (D_0\boldsymbol{\nabla}\cdot\mathbf{r}' - \mathbf{r}'\cdot\boldsymbol{\nabla}D_0)/2$ is in the same form as each of the components of $\mathbf{W}$. It may be possible to interpret D_T as a "phase-independent forcing" of a phase-independent pseudomomentum M.

[6] Since M and $\mathbf{W}$ are independent of wave phase, the space and time derivatives that explicitly appear in (31), in effect, represent slow variations on the spatial and temporal scales of a wave packet, respectively, which are much larger than the wavelengths and periods of components that compose the wave packet.

Unauthenticated | Downloaded 08/23/22 02:00 PM UTC

where C_P is again the phase speed in the direction of the basic flow $\mathbf{U} = (U, V, 0)^{\mathrm{T}}$, and the three-dimensional divergence and horizontal gradient operators are expressed as

$$\boldsymbol{\nabla}\cdot = \left(\frac{1}{a\cos\phi}\frac{\partial}{\partial\lambda}, \frac{1}{a\cos\phi}\frac{\partial}{\partial\phi}\cos\phi, \frac{\partial}{\partial z}\right)^{\mathrm{T}} \quad \text{and}$$

$$\boldsymbol{\nabla}_H = \left(\frac{1}{a\cos\phi}\frac{\partial}{\partial\lambda}, \frac{1}{a}\frac{\partial}{\partial\phi}, 0\right)^{\mathrm{T}},$$

respectively.

3. Examples

a. Stationary eddies in numerical simulations

As the first example of applications of our wave-activity flux **W**, we briefly refer to Enomoto and Matsuda (1999), who examined the behavior of stationary Rossby waves around critical latitudes through numerical integrations of the two-dimensional nondivergent barotropic vorticity equation on a sphere. In one of their experiments, Rossby waves are forced by a localized divergence centered at (40°N, 90°E) in the exit region of a midlatitude westerly jet (Fig. 1a). On the map of the response streamfunction (ψ') 14 days after the activation of the forcing (Fig. 1b), a wave train emanating downstream from the forcing region appears to be split into two branches, each of which is approximately along a great circle as in a theoretical argument by Hoskins and Karoly (1981). The wave-activity flux **W**, estimated from ψ' with $C_P = 0$ prescribed in (C5), clearly illustrates the wave propagation along these two branches (Fig. 1c). Along the northern branch, **W** across the diffluent westerlies converges into the weak-westerly region along the southern flank of the jet entrance. The flux along the southern branch delineates that the wave activity indeed propagates through an equatorial westerly duct and then across the diffluent Southern Hemisphere (SH) westerlies until it finally converges into a weak-westerly region along the northern flank of the southern jet. Our flux diverges out of the forcing region in the NH and traces positive and negative ψ' centers along the branch even beyond the equator, which clearly indicates that the ψ' centers in the SH are indeed associated with the wave train forced in the midlatitude NH.[7] Since zonal asymmetries in the background flow in that experiment are not very strong, $\mathbf{F}_s$ derived in P85 for a zonally *uniform* basic flow can depict the above-mentioned propagation over the extratropics in a very similar manner (not shown). However, $\mathbf{F}_s$ cannot be applied, in theory, to the tropical westerly duct where the *zonal-mean* flow is easterly, and hence it cannot illustrate the wave-packet propagation across the Tropics. An important aspect evident in Figs. 1c and 1d is that **W** and $\boldsymbol{\nabla}\cdot\mathbf{W}$ are almost free from the half-wavelength component of stationary Rossby waves. Another

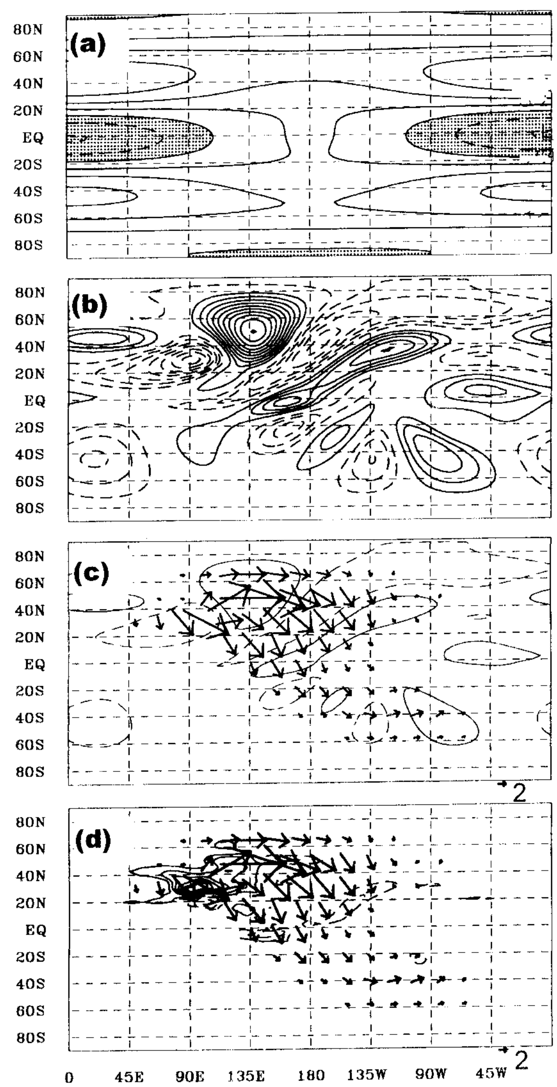

FIG. 1. (a) Zonal wind velocity of the basic state for a barotropic model experiment by Enomoto and Matsuda (1999). Contoured for every 10 m s^{-1} and the easterlies are shaded. (b) Day-14 streamfunction response ψ' (every 10^6 m^2 s^{-1}; dashed for negative values) to divergence forcing centered at (40°N, 90°E). (c) Corresponding wave-activity flux **W** (arrow), superimposed on contours for $\psi' = \pm 2 \times 10^6$ m^2 s^{-1}. Scaling for the arrows is given near the lower-right corner (unit: m^2 s^{-2}). (d) Wave-activity flux **W** (arrow) superimposed on contours for divergence of **W**. Contoured for every $\pm 2.0 \times 10^{-6}$ m s^{-2}; zero contours are omitted and dashed lines are for negative values (i.e., convergence). Each of the above evaluations was made by setting $C_P = 0$.

[7] There are some streamfunction anomalies in part of the Tropics where the basic flow is easterly and hence stationary Rossby waves cannot exist in the linear theory. Those anomalies are not associated with the wave-packet propagation from the forcing region. They appear to be associated with patches of relative vorticity that are cut off from the westerly duct due to wave breaking and then advected by the background easterlies. See Enomoto and Matsuda (1999) for details.

Unauthenticated | Downloaded 08/23/22 02:00 PM UTC

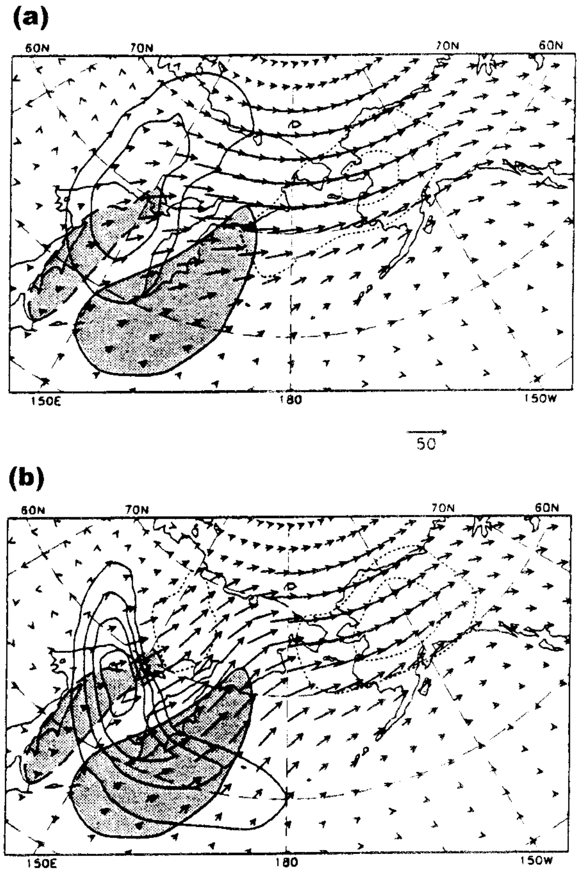

FIG. 2. Wave-activity fluxes associated with a stationary Rossby wave train forced thermally by anomalous surface heat fluxes in association with anomalous sea-ice cover within the Sea of Okhotsk, in a simulation by Honda et al. (1999). Horizontal components of $\mathbf{F}_s$ of P85 and $\mathbf{W}$ defined in (C5) were evaluated on pressure surfaces and then averaged between the 200- and 500-hPa levels: (a) $\mathbf{F}_s$ (arrows) and $\nabla_H \cdot \mathbf{F}_s$ (contoured), (b) $\mathbf{W}$ (arrows) and $\nabla_H \cdot \mathbf{W}$ (contoured). Scaling for the arrows is given between the panels. Light solid and dashed lines indicate the flux divergence and convergence, respectively. Contour interval: 1.0×10^{-5} m s^{-2}; zero lines are omitted. In the shaded regions surrounded by heavy solid and dashed lines, anomalies of surface turbulent heat fluxes into the atmosphere are significantly positive and negative, respectively, exceeding 200 W m^{-2} in magnitude.

important aspect is that $\mathbf{W}$ is, in general, almost perpendicular to phase lines of the waves as represented by the $\psi' = 0$ contours. Apparently, $\mathbf{W}$ tends to be parallel to the local group velocity of stationary Rossby waves, as shown theoretically in the previous section.

Another application of $\mathbf{W}$ to a model-simulated stationary response is found in Honda et al. (1999), who examined a stationary Rossby wave train forced thermally by anomalous surface heat fluxes in association with abnormal sea-ice cover within the Sea of Okhotsk. They compared $\mathbf{W}$ with $\mathbf{F}_s$ of P85 both estimated from the stationary response (Fig. 2). In the upper troposphere, $\mathbf{W}$ is strongly divergent right over a pair of the primary cooling and heating sources in the Sea of Okhotsk and to the east of it, respectively. Compared to $\nabla_H \cdot \mathbf{W}$, $\nabla_H \cdot \mathbf{F}_s$ is shifted to the west and spreads over eastern Siberia, where no significant heating or cooling source is present. Hence, in this example, $\nabla \cdot \mathbf{W}$ leads to a more reasonable estimation of the wave forcing region than $\nabla \cdot \mathbf{F}_s$ of P85 does.

b. Observed stationary eddies associated with blocking

Blocking highs are associated with high-amplitude, quasi-stationary anticyclonic anomalies that give rise to prolonged abnormal weather situations. In most cases a blocking anticyclone decays by releasing accumulated wave activity toward downstream in the form of a stationary Rossby wave train. A number of studies indicated that blocking formation is due primarily to local feedbacks from migratory synoptic-scale eddies. Recent studies have demonstrated, however, that in some locations a converging wave-activity flux associated with an incoming stationary Rossby wave train is of primary importance in blocking formation (e.g., Nakamura et al. 1997). Hence, diagnosing $\nabla_H \cdot \mathbf{W}$ associated with stationary Rossby waves on a meandering mean flow may be insightful for understanding the dynamics that underlies the blocking formation. One may argue that applying a wave-activity flux to a blocking phenomenon is inappropriate because a blocking high itself consists of high-amplitude anomalies. With their nonlinearities, the plane-wave assumption utilized in deriving $\mathbf{W}$ must break down in the vicinity of the blocking center. Still, a stationary Rossby wave train emanating from a blocking ridge or an incoming one from upstream to the ridge should exhibit nonlinearity to a much lesser degree, and hence they may be regarded as linear waves suited for applying $\mathbf{W}$.

We use twice-daily gridded fields of geopotential height at the 250-hPa level, based on the operational analyses by the National Meteorological Center [now known as the National Centers for Environmental Prediction (NCEP)] for 1965–92. The dataset was obtained from the National Center for Atmospheric Research (NCAR) Data Library. As in Nakamura et al. (1997), these fields were composited relative to the peak times of the 15 strongest blocking events observed around a given location in the 27 winter seasons (mid-November–mid-March). Before compositing, a low-pass filter with a cutoff period of 8 days was applied to the data time series, in order to isolate quasi-stationary eddies from migratory, higher-frequency transients. The basic state for the quasi-stationary eddies was defined as the 27-winter mean (Fig. 3). Departures of the filtered data from this mean state represent circulation anomalies associated with a blocking high and accompanied stationary wave trains. We use $\mathbf{W}$ on the pressure coordinate whose expression is given in appendix C. For simplicity, wind fields were approximated by the local geostrophic winds.

In Fig. 4, we plot the horizontal component of $\mathbf{W}$ and

Unauthenticated | Downloaded 08/23/22 02:00 PM UTC

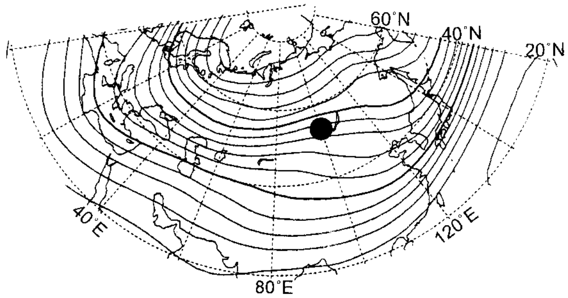

FIG. 3. Climatological-mean 250-hPa height (m) in winter (mid-Nov–mid-Mar) for 1965–92. Contour interval is 100. Heavy lines indicate 10 000 and 10 500. The closed circle corresponds to the composited blocking center at (54°N, 100°E).

its divergence ($\nabla_H \cdot \mathbf{W}$) based on the composite blocking flow centered around (54°N, 100°E). It is obvious that $\mathbf{W}$ and $\nabla_H \cdot \mathbf{W}$ both exhibit little oscillatory component with one-half wavelength. During the development (day -2) of the blocking ridge, quasi-stationary height anomalies are evident near (60°N, 40°E) upstream of the ridge. The associated **W** is dominantly eastward and nearly perpendicular to the height anomaly contours. The flux is converging into the amplifying blocking ridge and divergent upstream, which is suggestive of a particular importance of a converging wave-activity flux associated with an incoming stationary Rossby wave train in the blocking formation over Siberia, as Nakamura (1994) and Nakamura et al. (1997) demonstrated for a European blocking ridge.[8] During the breakdown of the block, **W** diverges out of the blocking center and converges into newly developing cyclonic anomalies downstream.

In Fig. 4, we also compare **W** with $\mathbf{F}_s$ defined in P85 for a zonally uniform basic flow. Neither $\mathbf{F}_s$ nor our flux **W** apparently exhibits an oscillatory component on a scale of one-half wavelength, and $\mathbf{F}_s$ and **W** are distributed similarly at a first glance. A close inspection

[8] We also applied **W** to the low-pass-filtered height anomalies composited for the 15 strongest blocking anticyclones observed over Europe (54°N, 10°E). We confirmed the findings of Nakamura (1994) and Nakamura et al. (1997) based on the flux of P86 artificially smoothed in space.

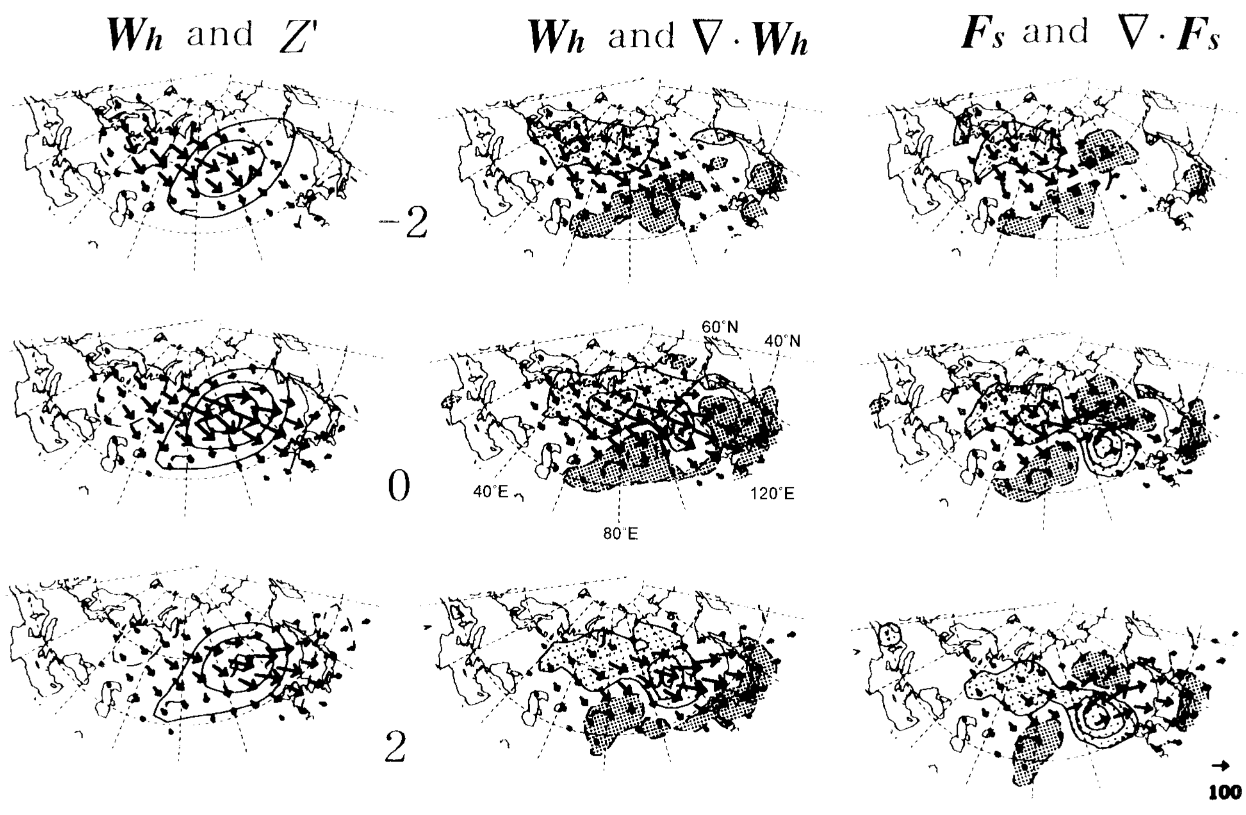

FIG. 4. Composite time evolution associated with the 15 strongest blocking events at the 250-hPa level around (54°N, 100°E) for -2, 0, and $+2$ days relative to the peak blocking time (from top to bottom; negative and positive values signify the amplification and decay stages, respectively). Presented are (left column) the horizontal component of our flux **W** with arrows based on low-pass-filtered 250-hPa height anomalies Z' as contoured, (middle column) **W** with arrows superimposed on its horizontal divergence with shading, and (right column) horizontal component of $\mathbf{F}_s$ of P85 with arrows and its divergence with shading. Here Z' is normalized by sin(45°N)/sin(lat). Contour intervals: every 100 m for Z' (dashed for negative values); ±0.25, ±0.75, . . . (10^{-4} m s^{-2}) for flux divergence; zero contours are omitted in all panels. Heavy and light shading signify the flux convergence and divergence, respectively. Scaling for arrows is given near the lower-right panel (unit: m^2 s^{-2}).

Unauthenticated | Downloaded 08/23/22 02:00 PM UTC

reveals, however, that **W** exhibits a stronger meridional component than $\mathbf{F}_s$ over central and eastern Siberia (Fig. 4), where V is significantly southward upstream of a climatological-mean trough (Fig. 3). The lack of contributions of V seems to cause an unrealistic undulation in the stream of $\mathbf{F}_s$ (i.e., corresponding $\mathbf{C}_g$) around the blocking ridge. Farther to the east, $\mathbf{F}_s$ penetrates into the trough, which is again unrealistic, whereas **W** is suppressed within the trough and its main stream follows the jet axis detouring to the south of the trough. Hence, **W** follows the meandering basic flow better than $\mathbf{F}_s$, thus better representing the advective nature of $\mathbf{C}_g$ of stationary Rossby waves. The tendency that **W** is systematically stronger than $\mathbf{F}_s$ over Siberia reflects the fact that the background westerlies are substantially stronger there than the zonal average.

Another comparison between **W** and $\mathbf{F}_s$ was presented in TN97, who applied these fluxes to the low-pass-filtered circulation anomalies composited for the 15 strongest blocking anticyclones around (56°N, 160°W). They showed that **W** and $\mathbf{F}_s$, including their divergence patterns, were nearly phase-independent. It was shown again that **W** follows the meandering mean westerlies better than $\mathbf{F}_s$.

c. Observed migratory eddies: A baroclinic wave packet

In this subsection, we present an example of our wave-activity flux applied to migratory eddies. The data we use are 12-hourly gridded fields of geopotential height and temperature based on the NCEP–NCAR reanalyses. A high-pass filter with a cutoff period of 8 days was applied to the data time series, in order to extract migratory, high-frequency transient disturbances. As in the previous subsection, **W** was evaluated on pressure surfaces. We focus on the period around 20 November 1983, when strong high-frequency disturbances were observed over the North Pacific.

Since the static stability of basic state is assumed to be uniform on a pressure surface in QG scaling, interpretations of **W** may be somewhat complicated at the 250-hPa level where a tropopause intersection often occurs. In the lower tropopause levels, on the other hand, a tropopause intersection is much less frequent. However, a region where M and hence **W** are well defined is much narrower horizontally, because these pressure levels are close to the steering level of the baroclinic disturbances. Thus, the 300-hPa level was chosen for plotting the horizontal distribution of **W**, in order both to suppress influence of the intersecting tropopause to some extent and to depict horizontal wave propagation reasonably well within substantial part of the analysis domain.

Figure 5 shows the 8-day low-pass-filtered 300-hPa height for that day, regarded as the basic state on which those high-frequency disturbances are embedded. A strong westerly jet over the midlatitude North Pacific, where ($|\mathbf{U}| - C_P$) exceeds a certain positive value, say 2.0 (m s^{-1}), approximately defines a ''wave guide'' for the migratory eddies.

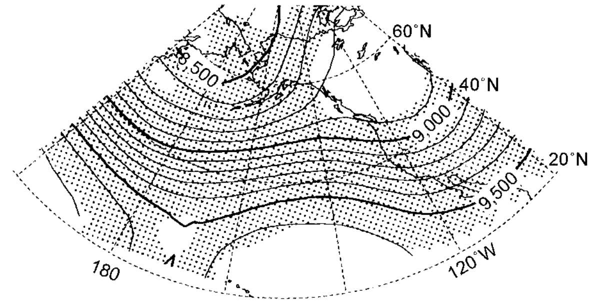

FIG. 5. Basic state for migratory disturbances, as defined by 8-day low-pass-filtered 300-hPa height field at 0000 UTC on 20 Nov 1983. Contour interval is 100 m. Heavy lines denote 8500, 9000, and 9500 m. Regions where $|\mathbf{U}| - C_P < 2.0$ m s^{-1} are shaded.

Before computing **W** based on (C5) with ψ'_p evaluated from the high-pass-filtered temperature fluctuations, we estimated C_P at each grid point in the following manner. First, we computed the correlation coefficients of the high-pass-filtered 250-hPa geopotential height time series between a particular grid point and other grid points over the 21-day period centered on the day of interest, imposing a lag of -12 h. Then, the correlation coefficients were calculated in the same manner but this time with a lag of $+12$ h imposed. Next, the actual phase propagation was estimated by tracing the maximum positive correlation center on the one-point correlation maps thus constructed from the negative to positive lag (Blackmon et al. 1984). Finally, the local value of C_P for that grid point was determined as the projection of this phase propagation onto the direction of the local basic flow **U**.

In Fig. 6, we plot **W** to show snapshots of a ''baroclinic wave packet'' at the 300-hPa level. Each of the wave components (i.e., highs and lows) move eastward with $C_P \approx 10$ (m s^{-1}), while their envelope appears to propagate eastward much faster accompanied by the rapid decay of a cyclonic anomaly center over the western Pacific. These features may be indicative of downstream development of the disturbances (e.g., Chang and Orlanski 1993) although it may be more or less underestimated here in the high-pass-filtered fields. Over the Gulf of Alaska the stream of **W** splits into two branches, following the split mean flow. While part of the wave activity is propagating into higher latitudes, most of the activity propagates southeastward along the main branch of the westerly jet. A region of strong upper-level divergence ($\nabla_H \cdot \mathbf{W}$) almost coincides with that of the strongest upward **W** at the 600-hPa level[9] (Fig. 6). This ''wave source'' region gradually weakens, as it quickly

[9] The units of the vertical component of **W** shown in Fig. 2 of TN97 should be 10^{-1} (Pa m s^{-2}). Also, the unit is different from that of P85 because of the difference in the vertical coordinate (p vs log$p$).

Unauthenticated | Downloaded 08/23/22 02:00 PM UTC

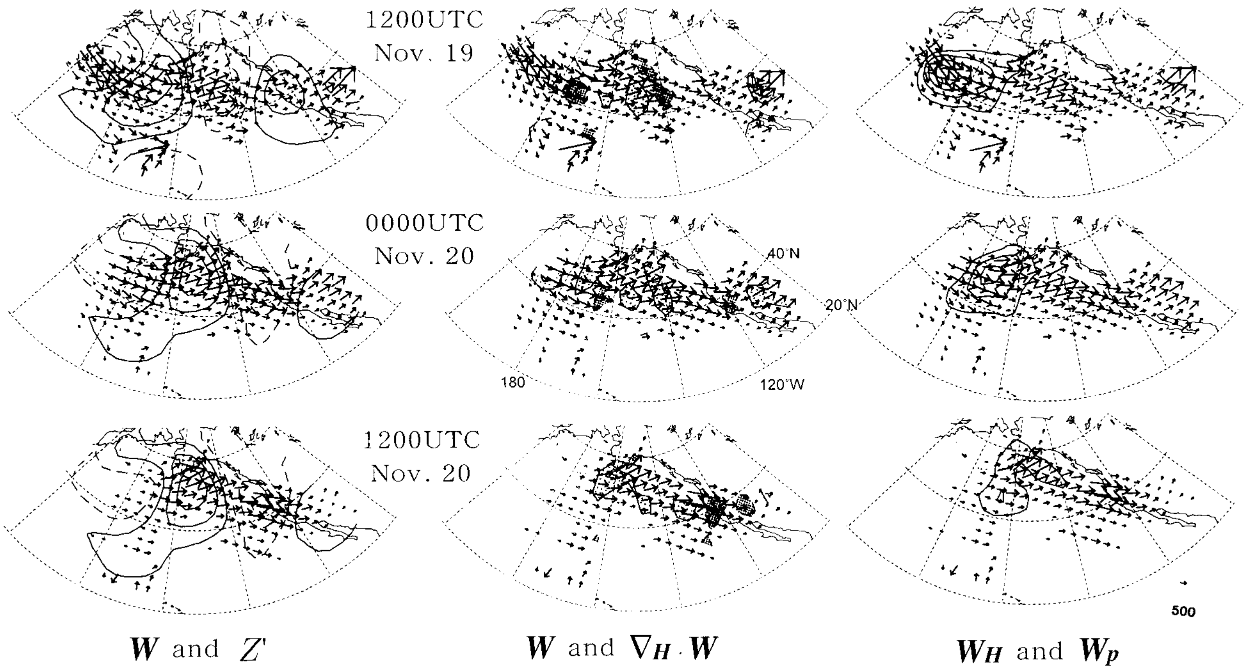

FIG. 6. Time sequence of (left column) 8-day high-pass-filtered 300-hPa height (Z'), superimposed on the horizontal component of **W** with arrows, (middle column) horizontal component of **W** with arrows and its divergence/convergence with contours, and (right column) horizontal component of **W** with arrows superimposed on the vertical component of 600 hPa with contours. The sequence begins at 1200 UTC on 19 Nov 1983 with 12-h intervals (from top to bottom). Here Z' is contoured for every 100 m from 50 m and dashed for negative values, and $\boldsymbol{\nabla}_H \cdot \mathbf{W}$ is contoured for every 8.0×10^{-4} m s^{-2}. Light shading with solid lines and heavy shading with dashed lines denote the divergence and convergence, respectively. The vertical component of **W** is contoured for every 5.0 Pa m s^{-2}. Solid and dashed lines indicate where the flux is upward and downward, respectively. Scaling of **W** is given near the lower panel (unit: m^2 s^{-2}).

moves eastward following the wave packet toward the region where the basic-state baroclinicity is weaker. Another wave source region seems to be around (50°N, 150°W), just upstream of the split of the jet. In Fig. 6, **W** and $\boldsymbol{\nabla}_H \cdot \mathbf{W}$ appear to be somewhat noisier than in the applications to stationary eddies (as in Fig. 4). Nevertheless, the suppression of half-wavelength noise and the dominance of the wave-packet signal on scales of a wavelength or larger are both apparent in Fig. 6, which manifest the greatest advantage of our flux **W**.

It is clear in the zonal and meridional cross sections (Figs. 7a and 7b) that the wave-activity flux are dominantly upward in the mid- to upper troposphere over the primary wave source region between the date line and 160°W, indicating conversion of the available potential energy from the mean flow to the disturbances. From this ''source region'' the wave activity propagates dominantly eastward along the upper-tropospheric jet. Part of the wave activity appears to be propagating slightly upward and downward above and beneath of the 350-hPa level, respectively, around 155°W as if there were another wave source region, which is consistent with the distribution of $\boldsymbol{\nabla}_H \cdot \mathbf{W}$ shown in Fig. 6.

d. Validity assessment of the approximations

In the previous subsections, we applied an approximate conservation relation of the phase-independent wave-activity pseudomomentum M with its phase-independent flux **W** for QG eddies to simulated and observed data. In the derivation for the case where a basic flow is zonally inhomogeneous, we needed to assume that it is unforced and varying slowly in space, which corresponds to approximations, for example, of (12), (13), (17), (19), and (21) in section 2. In this section, we attempt to assess their validity in the individual applications in the previous subsections. Specifically, the following relation on the pressure coordinate is readily derived from (12), (13), (17), and (19):

$$\mathcal{L} \equiv \frac{1}{2}\left[\frac{\mathbf{u}' \cdot (\boldsymbol{\nabla}_H Q)}{|\boldsymbol{\nabla}_H Q|} q' - \frac{\mathbf{U} \cdot (\boldsymbol{\nabla}_H q')}{|\mathbf{U}|} \psi' \right. + \frac{1}{|\boldsymbol{\nabla}_H Q|} \boldsymbol{\nabla} \cdot \left(\frac{C_P q'^2}{2|\mathbf{U}|}\mathbf{U}\right) \left. + \frac{C_P}{(|\mathbf{U}| - C_P)} \frac{\mathbf{U}}{|\mathbf{U}|} \cdot \boldsymbol{\nabla} e \right] \approx \boldsymbol{\nabla} \cdot \mathbf{W}. \qquad (39)$$

The rhs of (39) has been derived from the lhs under the assumption of an unforced, slowly varying basic flow. However, we are not certain how reasonable this assumption is in our applications, for example, to the observed mean flow that undulates in the presence of the planetary waves. In the following, we attempt to assess

Unauthenticated | Downloaded 08/23/22 02:00 PM UTC

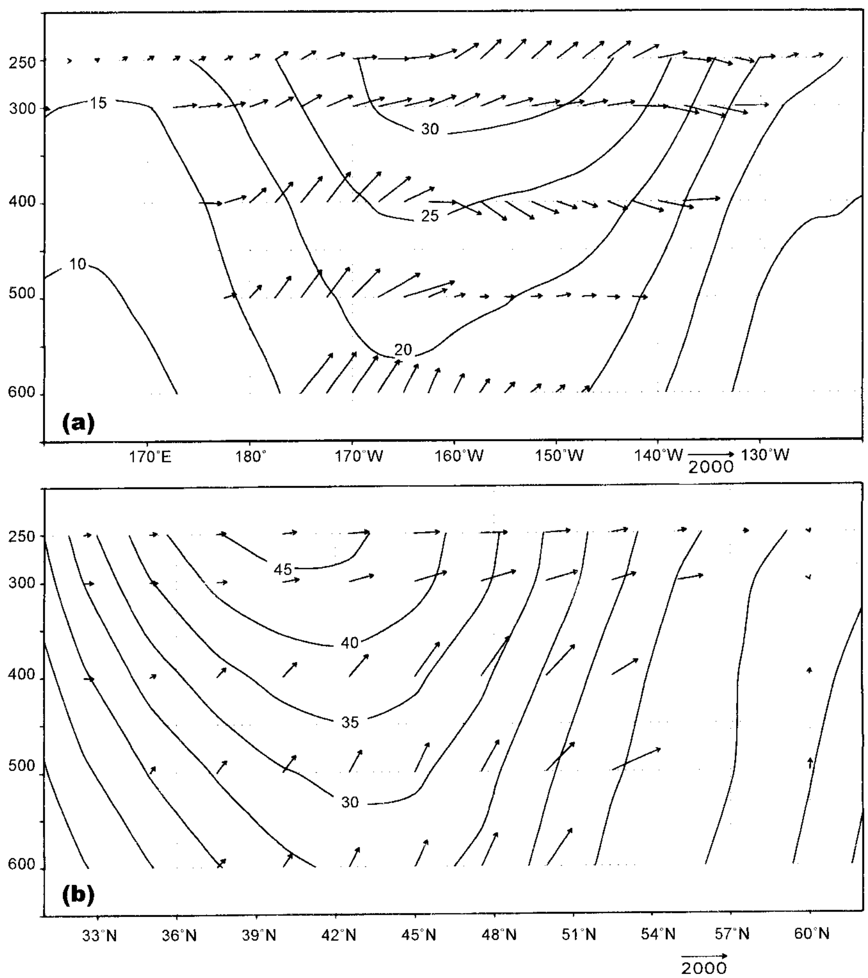

FIG. 7. (a) Zonal-vertical section along 50°N where the zonal and vertical components of **W** are plotted with arrows. (b) Meridional-vertical section along 170°W where the meridional and vertical components of **W** are plotted with arrows. In (a) and (b) the basic-state westerlies are superimposed with contours (every 5 m s^{-1}). Scaling of **W** is given just below the individual panels. (units: for horizontal component m^2 s^{-2}; for vertical component 10^{-2} Pa m s^{-2}). Note that M can be defined only in regions where $|\mathbf{U}| > C_P$.

the validity of that assumption based on the spherical version of the approximate relation (39). The two sides of (39), that is, $\mathcal{L}$ and $\nabla \cdot \mathbf{W}$, are distributed alike if the aforementioned assumption is reasonable. In our derivation we also neglected the residual term R, which is expressed on the pressure coordinate as

$$R = \left(\frac{\partial e}{\partial t} + \frac{U}{|\mathbf{U}|}C_P\frac{\partial e}{\partial x} + \frac{V}{|\mathbf{U}|}C_P\frac{\partial e}{\partial y}\right) + \psi'\left(\frac{\partial q'}{\partial t} + \frac{U}{|\mathbf{U}|}C_P\frac{\partial q'}{\partial x} + \frac{V}{|\mathbf{U}|}C_P\frac{\partial q'}{\partial y}\right), \quad (40)$$

under the assumption that the eddies are in the form of a plane wave on a β plane. We evaluate $\nabla \cdot \mathbf{W}$ and $R/2(|\mathbf{U}| - C_P)$ with the spherical version based on the actual data. If the latter (hereafter referred to as $\mathcal{R}$) is substantially less than the former ($\nabla \cdot \mathbf{W}$), our neglect of the residual term may be justified.

First, we evaluated the two sides of (39) at each grid point, based on the barotropic simulation by Enomoto and Matsuda (1999, see Fig. 1). In the evaluation, only the horizontal component was used and PV was replaced by the absolute vorticity. The patterns of $\mathcal{L}$ and $\nabla_H \cdot \mathbf{W}$ [i.e., rhs of (39)] are almost identical (Figs. 8a and 8b), indicating that the approximations adopted in our derivation are reasonable. Next, the dominance of $\nabla_H \cdot \mathbf{W}$ over the residual term $\mathcal{R}$ is checked by setting $C_P = 0$ in (40). Again, we evaluated the horizontal component only. It is apparent in Fig. 8c that $\mathcal{R}$ is indeed negligible compared to $\nabla_H \cdot \mathbf{W}$ all over the midlatitudes and even in a tropical westerly duct.

The same assessment as above was performed based on the composited height anomalies for the Siberian

Unauthenticated | Downloaded 08/23/22 02:00 PM UTC

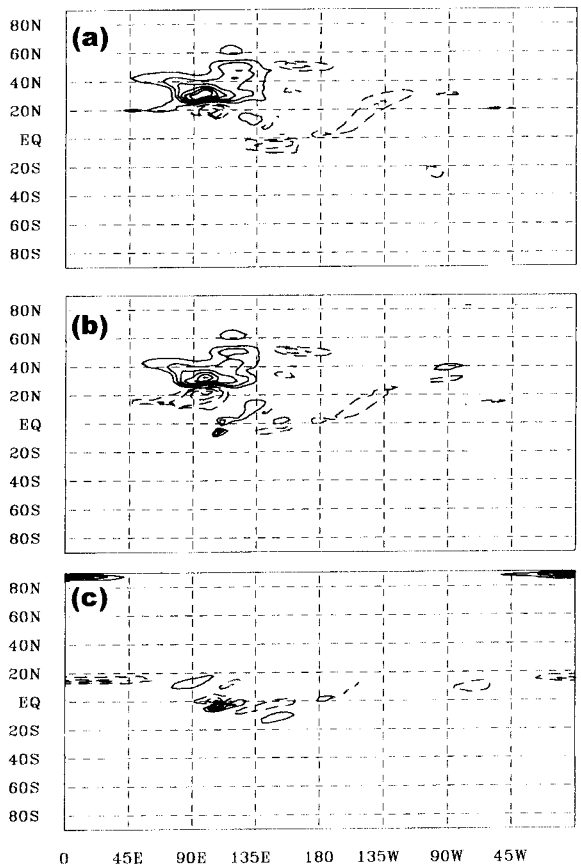

FIG. 8. (a) Divergence of **W**, (b) $\mathcal{L}$; i.e., lhs of (39) and (c) the residual term $\mathcal{R}$ in (40), all based on day-14 response of a barotropic model experiment by Enomoto and Matsuda (1999) as shown in Fig. 1. Each of the above evaluations was made by setting $C_p = 0$. Contoured for every $\pm 2.0 \times 10^{-6}$ m s^{-2}, zero contours are omitted in all panels, and dashed lines are for negative values (or convergence).

blocking. At each grid point, $\nabla_H \cdot \mathbf{W}$, $\mathcal{L}$, and $\mathcal{R}$ in (39) and (40) for the peak blocking time (lag = 0) were evaluated with the local geostrophic balance assumed. Since these stationary anomalies are nearly equivalent barotropic and hence **W** is almost horizontal, we again evaluated only the horizontal component in (39). Even at the peak time (lag = 0) when nonlinearities are the strongest, $\mathcal{L}$ and $\nabla_H \cdot \mathbf{W}$ are distributed alike and their values do not differ substantially (Figs. 9a and 9b). Furthermore, it is apparent in Figs. 9a and 9c that the $\mathcal{R}$ is negligible relative to $\nabla_H \cdot \mathbf{W}$. The same tendency appears also for other blocking composites for the Pacific and Europe, except in the vicinity of the blocking center where the plane-wave assumption breaks down due to strong nonlinearities. We should remember that uncertainties at a certain level are included in the above assessment, which arises from several assumptions made in our data manipulations. Still, it appears that our flux **W** presents a qualitatively correct snapshot of the propagation of a stationary wave packet, but the flux may be not suited for the exact evaluation of the local budget of *M*.

The pattern of our flux **W** and its three-dimensional divergence ($\nabla \cdot \mathbf{W}$) at the 300-hPa level associated with migratory synoptic-scale eddies are shown in Fig. 10a. Again, we use the data at 20 November 1983. We compare $\nabla \cdot \mathbf{W}$ with $\mathcal{L}$ shown in Fig. 10b to assess how reasonable the assumptions are for the basic flow. We find that their spatial patterns and their values are both similar, respectively. Therefore, the assumption of an unforced, slowly varying basic state seems to be valid, at least qualitatively. The residual term $\mathcal{R}$ shown in Fig. 10c tends to be negligible compared to $\nabla \cdot \mathbf{W}$ along the Pacific stormtrack, indicative of the validity of the almost-plane wave assumption for the high-pass-filtered disturbances. The residual term is noticeable only near the wave source region at the western edge of the wave packet.

4. Physical interpretations of phase-independent wave-activity fluxes

In section 2, we formulate a phase-independent wave-activity flux **W**. Though shown to be parallel to the local three-dimensional group velocity $\mathbf{C}_g$ of a Rossby wave packet, a rather complicated expression of the flux may make it difficult to intuitively relate it to the wave packet propagation mechanisms. In this section, we pre-

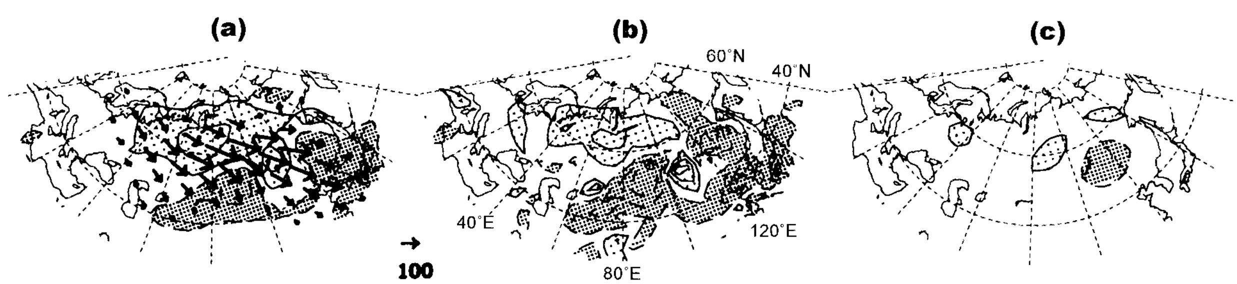

FIG. 9. (a) Horizontal component of **W** (arrows with scaling given near the lower-right panel; unit: m^2 s^{-2}) and its divergence (contoured and shaded), (b) $\mathcal{L}$ of (39); and (c) the residual term $\mathcal{R}$ evaluated on the basis of (40), all based on the composite low-pass-filtered evolution at the 250-hPa level for the 15 strongest blocking events around (54°N, 100°N), for the peak blocking time (see Fig. 4). Contoured for ± 0.25, ± 0.75, . . . (10^{-4} m s^{-2}; dashed for negative values) and zero contours are omitted in all panels. Heavy and light shading signifies negative (or convergence) and positive (or divergence) values, respectively.

Unauthenticated | Downloaded 08/23/22 02:00 PM UTC

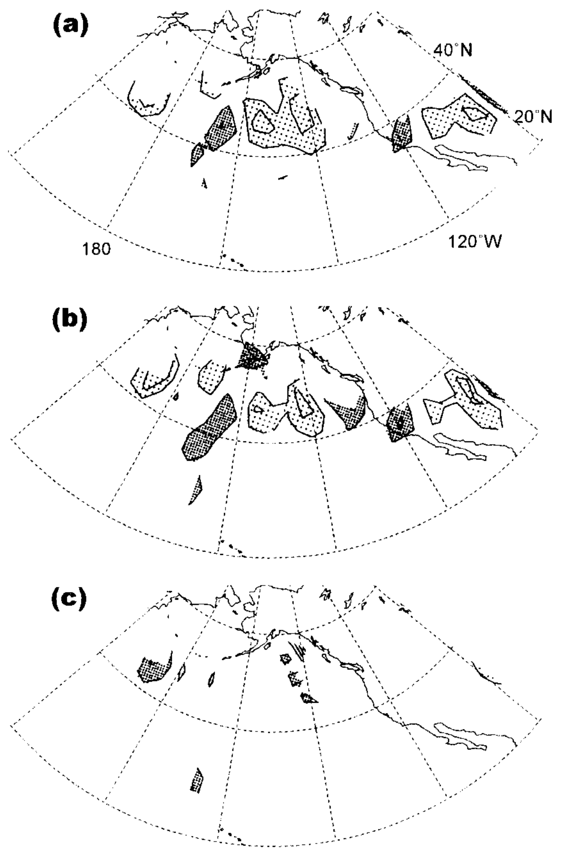

FIG. 10. Same as Fig. 9 but based on 8-day high-pass-filtered data at 0000 UTC on 20 Nov 1983 (see Fig. 6). (a) Three-dimensional divergence is plotted. Contoured for every 8.0 (10^{-4} m s^{-2}) and dashed for negative values. Zero contours are omitted. Heavy and light shading signifies negative (or convergence) and positive (or divergence) values, respectively.

sent an interpretation in which each term of the individual components of our flux or $\mathbf{F}_s$ of P85 is related to an explicit physical process involved in the wave packet propagation. We also formulate a set of generalized transformed Eulerian-mean (TEM) equations that represent instantaneous feedbacks from a propagating Rossby wave packet upon a basic flow on which the packet is embedded.

For simplicity, we consider disturbances propagating through a zonally uniform basic flow (U), for which pseudomomentum is exactly conserved. In this case, the following argument directly applies to $\mathbf{F}_s$ of P85 if the disturbances are stationary. A linearized QG equation of meridional momentum for the disturbances may be written as

$$\frac{\partial v'}{\partial t} + U\frac{\partial v'}{\partial x} + f(u' + u_{(a)}) = -\frac{\partial \phi'}{\partial x}, \qquad (41)$$

where $u_{(a)}$ is the Eulerian zonal ageostrophic flow associated with the disturbances and other quantities of the disturbances are denoted by primes. For unforced disturbances propagating zonally with phase speed c on a β plane, the above equation may be simplified as

$$(U - c)\frac{\partial v'}{\partial x} + f_0 u_{(a)} + \beta y u' = 0 \qquad (42)$$

(e.g., Holton 1992). Thus, an approximate relation $\psi'_{xx} = v'_x \simeq -f_0 u_{(a)}/(U - c)$ holds on and around ridge/trough lines associated with the disturbance. Likewise, from linearized equations of zonal momentum and thermodynamics, we obtain $\psi'_{xy} = -u'_x \simeq -f_0 v_{(a)}/(U - c)$ and $f_0\Theta_z\psi'_{xz}/N^2 = \theta'_x \simeq -\Theta_z w_{(a)}/(U - c)$, where $v_{(a)}$ and $w_{(a)}$ are the meridional and vertical ageostrophic motions associated with the disturbance, respectively. It follows that when $U > c$,

$$\left(-\psi'\psi'_{xx},\ -\psi'\psi'_{xy},\ -\frac{f_0^2}{N^2}\psi'\psi'_{xz}\right)^{\mathrm{T}} \simeq \frac{(\Phi' u_{(a)},\ \Phi' v_{(a)},\ \Phi' w_{(a)})^{\mathrm{T}}}{(U - c)}$$

holds on and around the ridge/trough lines, where Φ' denotes eddy geopotential. Therefore, the second term of each component of $\mathbf{F}_s$ is related to a three-dimensional ageostrophic geopotential flux that corresponds to the rate of working by the pressure force in the direction of $\mathbf{C}_g$ of a Rossby wave packet acting most strongly on the ridge/trough lines of the wave (Figs. 11a and 11b). In fact, it can readily be shown that the vector $[-\psi'\psi'_{xx}, -\psi'\psi'_{xy}, -(f_0^2/N^2)\psi'\psi'_{xz}]^{\mathrm{T}}$ points to the direction of $\mathbf{C}_g$ in the almost plane-wave limit.

We next consider the first term of each component of $\mathbf{F}_s$ (or $\mathbf{W}_s$). We begin with an interpretation of v'^2, relating it to wave-packet propagation in the zonal direction (in Fig. 11c). A meridional flux of the meridional momentum (v'^2) at point E on a node line of the ψ' field acts to induce the southward and northward geostrophic motions to the south (point B) and north (point D), respectively. Due to the nondivergent nature of the geostrophic flow, compensating westerly and easterly accelerations must occur to the west (point A) and east (point C). These accelerations at points A and C manifest the westward transport of the second-order westerly momentum, acting most strongly on node lines of the ψ' field, in the direction opposite to the eastward group velocity of the wave packet. An interpretation of $u'v'$ in the meridional component of $\mathbf{F}_s$ (or $\mathbf{W}_s$) is more straightforward. It represents the meridional transport of the second-order westerly momentum in the direction opposite to the meridional group velocity (Fig. 11c). The vertical component of $\mathbf{F}_s$ (or $\mathbf{W}_s$) includes the meridional temperature flux $v'\theta'$. For an upward propagating wave packet, the flux is poleward that acts to reduce the vertical westerly shear in a basic state (Fig. 11b), resulting in the downward transport of the second-order mean westerly momentum. Therefore, the first term of $\mathbf{F}_s$ including eddy momentum and heat fluxes represents the systematic ''backward'' transport of the

Unauthenticated | Downloaded 08/23/22 02:00 PM UTC

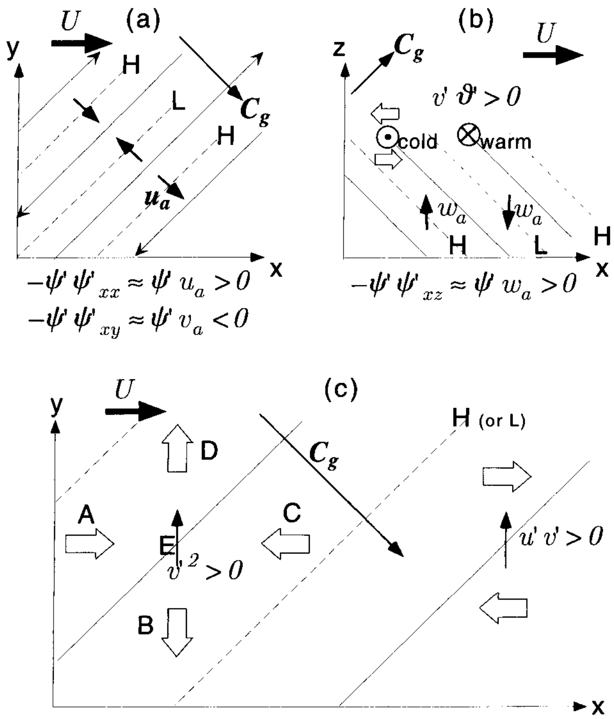

FIG. 11. Schematic diagrams for explanations of an instantaneous Rossby wave-packet propagation mechanism. In each diagram, thin solid lines denote node lines in the perturbation streamfunction (ψ') field at which perturbation QG flows are strongest, and thin dashed lines denote ridge (H)/trough (L) lines. Arrows with **U** and $\mathbf{C}_g$ signify the mean westerly flow and group velocity of the wave packet, respectively. (a) Horizontal ageostrophic flows ($\mathbf{u}_a$) associated with a wave-packet propagation, which aligned coherently on the ridge/trough lines and parallel to the horizontal group velocity. Thin arrows indicate the direction of the perturbation geostrophic flows. (b) Zonal-vertical section of an upward propagating Rossby wave packet. Short arrows with w_a indicate vertical (ageostrophic) motions aligned on the ridge/trough lines in association with wave packet. Open arrows signify the second-order acceleration of the mean westerly flow as a result of systematic poleward heat transport strongest on the node lines. (c) Second-order mean flow accelerations (indicated with open arrows) induced by eddy momentum transport (v'^2 on left and $u'v'$ on right). See text for more details.

mean westerly momentum that occurs mainly around the node lines of the ψ' field associated with a propagating Rossby wave packet.

The above arguments can readily be extended to **W** (or $\mathbf{W}_s$) applicable to wave-packet propagation through a zonally asymmetric basic flow. Thus, a snapshot of a Rossby wave-packet propagation can be represented as a superposition of the aforementioned two ‘‘complementary’’ dynamical processes involved in the propagation. It also becomes apparent that they exhibit different dependencies of the wave phase. Specifically, in the almost plane-wave limit of $\psi' = \psi_0 \sin(kx + ly + mz - \omega t)$, the ageostrophic flux of geopotential on ridge/trough lines of the ψ' field and the systematic backward transport of the mean ‘‘westerly’’ momentum on the node lines are proportional to sine squared and cosine squared of the wave phase, respectively. Hence, an appropriate combination of those two processes as in $\mathbf{F}_s$ and **W** leads to the elimination of their phase dependencies.

Finally, we consider interactions of QG eddies with a basic flow on which they are embedded. We follow the derivation of P86, but unlike P86, we utilize our phase-independent wave-activity flux **W**, so that instantaneous eddy feedbacks on the basic flow can also be independent of the wave phase. We begin with an $O(\epsilon^2)$ equation of an instantaneous tendency in the westerly momentum of the basic state on an f plane, which may be written as

$$\frac{D^{(0)}U^{(2)}}{Dt} - fV^{(2)} + \frac{\partial \Phi^{(2)}}{\partial x} = -\frac{\partial}{\partial x}u'^2 - \frac{\partial}{\partial y}u'v' = \frac{\partial}{\partial x}\psi'\psi'_{yy} - \frac{\partial}{\partial y}\psi'\psi'_{xy}, \quad (43)$$

where the superscript (2) denotes second-order modifications of the basic state and $D^{(0)}U^{(2)}/Dt \equiv \partial U^{(2)}/\partial t + (\mathbf{U} \cdot \boldsymbol{\nabla})U^{(2)} + (\mathbf{U}^{(2)} \cdot \boldsymbol{\nabla})U$. Note that the two expressions on the rhs of (43) are both phase-independent for almost plane-wave limit.[10] Combining these two equivalent expressions, we can write the eddy forcing term in a flux-divergence form:

$$\frac{D^{(0)}U^{(2)}}{Dt} - fV^{(2)} + \frac{\partial \Phi^{(2)}}{\partial x} = \frac{1}{2}\frac{\partial}{\partial x}(-u'^2 + \psi'\psi'_{yy}) - \frac{1}{2}\frac{\partial}{\partial y}(u'v' + \psi'\psi'_{xy}). \quad (44)$$

We stress that not only rhs of (44) but also each term of eddy flux component itself (within parentheses) is now independent of the wave phase. After simple manipulations, the baroclinic component of the eddy feedback can also be incorporated into (44) as

$$\begin{aligned}\frac{D^{(0)}U^{(2)}}{Dt} - fV^{(2)} + \frac{\partial \Phi^{(2)}}{\partial x} &= \frac{1}{2}(\psi'_x q' - \psi' q'_x) \\ &\quad - \frac{1}{2}\frac{\partial}{\partial x}[(\psi'^2_x - \psi'\psi'_{xx}) + (\psi'^2_y - \psi'\psi'_{yy})] \\ &\quad - \frac{1}{2p}\frac{\partial}{\partial z}p\left[\frac{f_0^2}{N^2}(\psi'_x\psi'_z - \psi'\psi'_{xz})\right].\end{aligned}$$

Likewise, equations of instantaneous second-order tendencies in the basic-state meridional momentum and potential temperature have been derived. Unifying these equations, the second-order tendency equations for the basic-state momentum and thermal fields may be expressed as follows:

[10] Therefore, derivatives in rhs of (43) indicate slow variations on the spatial and temporal scales of the wave packet, as in the same manner as in (31).

Unauthenticated | Downloaded 08/23/22 02:00 PM UTC

$$\frac{D^{(0)}\mathbf{U}^{(2)}}{Dt} - f\mathbf{k} \times \mathbf{U}^*_{(a)} = \mathbf{J} + \mathbf{X}, \tag{45}$$

$$\frac{D^{(0)}\Theta^{(2)}}{Dt} + W^*_{(a)}\frac{d\Theta}{dz} = Q, \tag{46}$$

where $\mathbf{X}$ and Q are nonconservative terms proportional to frictional force and diabatic heating, respectively. This system may be viewed as an extension of the standard TEM set defined on the meridional plane in a zonally averaged form, which was introduced by Andrews and McIntyre (1976), to the three-dimensional circulation in a phase-independent form. The vector $\mathbf{J}$ in (45) represents the eddy-induced forcing acting on the basic flow, which may be expressed in a phase-independent form as

$$\begin{aligned}\mathbf{J} &= -\frac{p}{2}\mathbf{k} \times (\mathbf{u}'q' - \psi'\mathbf{k} \times \boldsymbol{\nabla}_H q') \\ &\equiv -\frac{p}{2}\mathbf{k} \times \mathbf{P}.\end{aligned} \tag{47}$$

The vector $\mathbf{U}^*_a$ in (45) denotes a phase-independent three-dimensional residual ageostrophic circulation defined as

$$\mathbf{U}^*_{(a)} = (U^*_{(a)}, V^*_{(a)}, W^*_{(a)})^{\mathrm{T}} = \mathbf{U}^{(2)}_{(a)} + \frac{1}{p}\boldsymbol{\nabla} \times p\mathbf{R}, \tag{48}$$

where $\mathbf{U}^{(2)}_{(a)} = (U^{(2)}_{(a)}, V^{(2)}_{(a)}, W^{(2)}_{(a)})^{\mathrm{T}}$ is the second-order Eulerian ageostrophic flow. The second term on the rhs of (48), which may be related to the Stokes drift in the limit of small wave amplitude, includes the phase-independent vector $\mathbf{R}$ given by

$$\mathbf{R} = \frac{1}{2}\begin{pmatrix} -(v'\theta' - \psi'\theta'_x)/\Theta_z \\ (u'\theta' + \psi'\theta'_y)/\Theta_z \\ [(v'^2 - \psi'\psi'_{xx}) + (u'^2 - \psi'\psi'_{yy})]/f \end{pmatrix}. \tag{49}$$

These relations (45), (46), (47), (48), and (49) are in correspondence to (4.3), (4.4), (4.5), and (4.6) in P86, which are expressed in a time-averaged form and therefore inappropriate for stationary eddies. Our relations, in contrast, are expressed in a phase-independent form without any averaging required. They can therefore be used for evaluating instantaneous feedback forcing on the mean flow induced by a wave packet propagating through it, regardless of whether the packet consists of migratory or stationary eddies.

With a unit vector $\mathbf{s}$ normal to the PV gradient ($\boldsymbol{\nabla}_H Q$) defined as $\mathbf{s} \equiv \mathbf{k} \times \mathbf{n}$, an alternative expression of $\mathbf{J}$ may be given by

$$\mathbf{J} = -\frac{p}{2}[(\mathbf{P} \cdot \mathbf{n})\mathbf{s} - (\mathbf{P} \cdot \mathbf{s})\mathbf{n}]. \tag{50}$$

From (13), (19) and the relation of $\mathbf{W}_s \equiv (\mathbf{E} + \mathbf{H})/2$, the following approximate relation may be obtained

$$\boldsymbol{\nabla} \cdot \mathbf{W}_s \approx \frac{p}{2}\mathbf{n} \cdot (\mathbf{u}'q' - \psi'\mathbf{k} \times \boldsymbol{\nabla}_H q') = \frac{p}{2}\mathbf{P} \cdot \mathbf{n} \tag{51}$$

for an unforced basic state on a β plane. The first term on the rhs of (50) is related to $\boldsymbol{\nabla} \cdot \mathbf{W}_s$. It indicates instantaneous acceleration of a mean flow that a three-dimensionally propagating Rossby wave packet induces through the effect that corresponds to downgradient and upgradient fluxes of PV at the leading and trailing edges of the wave packet, respectively. Note that $\boldsymbol{\nabla} \cdot \mathbf{W}_s$ contributes to the mean-flow acceleration only in the direction along basic-state PV contours, but $\boldsymbol{\nabla} \cdot \mathbf{W}_s$ does not represent the total eddy-induced feedback, as pointed out by P86.

Our expression of a three-dimensional residual ageostrophic circulation is somewhat different from the corresponding expressions derived in P86 and Trenberth (1986), with respect particularly to the vertical component of $\mathbf{R}$ and its counterparts. The differences can be attributed partly to a distinction between our instantaneous phase-independent form and their time-averaged form. It can be attributed also to another distinction that eddy feedbacks in our formulation are evaluated on a coordinate system moving with wave *phase speed*, whereas the feedbacks in their formulations are on a coordinate system moving with a *basic flow*. Note that the vertical component $\mathbf{R}$ contributes to the horizontal residual motion in the TEM framework. Thus, a specific expression of the residual circulation does depend upon a coordinate system on which the eddy feedbacks are evaluated and upon a particular definition of a wave-activity flux as well, although these expressions of the residual circulation reduce to a single form when zonally averaged.

5. Conclusions

We have derived an approximate conservation relation of the wave-activity pseudomomentum for QG eddies on a zonally varying basic flow through averaging neither in time nor in space. We have shown that a linear combination of quantities A and $\mathcal{E}$, that is, $(A + \mathcal{E})/2$, is a conservative quantity (M) that can be interpreted as a wave-activity density for QG eddies and is independent of the wave phase in the almost-plane wave limit. We consider that M is a generalization of the small-amplitude pseudomomentum $(q')^2/(2Q_y)$ to nonzonal flows. We also consider that our conservation relation is a generalization of conservation laws of pseudomomentum as defined by P85 and TN97 with its phase-independent flux for stationary eddies. We have shown that the flux $\mathbf{W}$ of M is also phase-independent and parallel to the local $\mathbf{C}_g$ in the WKB limit. Derived without any averaging, $\mathbf{W}$ can depict instantaneous three-dimensional wave-packet propagation. Thus, $\mathbf{W}$ may be a useful diagnostic tool for a snapshot analysis for either migratory and stationary disturbances prop-

Unauthenticated | Downloaded 08/23/22 02:00 PM UTC

agating through a zonally varying basic flow, which is its greatest advantage.

Furthermore, we have presented a physical interpretation of individual terms of our flux **W** and $\mathbf{F}_s$ in P85. They illuminate the following two dynamical aspects of Rossby wave-packet propagation: one is the systematic transport of basic-state westerly momentum in the form of eddy momentum and heat fluxes that are strongest along node lines of an eddy streamfunction field, and the other is an associated ageostrophic flux of geopotential strongest along trough/ridge lines, which is related to the rate of working by the pressure force in the direction of the local group velocity of a Rossby wave packet. Although only the former aspect appears explicitly in the conventional and extended E–P fluxes and the flux of P86, they can still represent wave-packet propagations because they are expressed in phase-averaged forms by zonal or time averaging. In the wave-activity fluxes of P85 and ours, those two aspects of the wave-packet propagation are combined in an explicit manner so as to eliminate their phase dependencies. We have shown that the flux $\mathbf{F}_s$ of P85 can be derived, as our flux **W**, through manipulations of both the eddy enstrophy and energy equations, whereas the conventional and extended E–P fluxes were derived only on the basis of the enstrophy conservation form.

We now discuss relationships of our conservation law with others. First, we attempt to clarify the meaning of the supplementary nondivergent flux **G**, introduced rather heuristically in P85 for ensuring the phase independency of a wave-activity flux $\mathbf{F}_s$. With phase speed $C_P = 0$ prescribed, we may rewrite (15) as follows

$$\frac{\partial A}{\partial t} + \boldsymbol{\nabla} \cdot \mathbf{F} = D_1; \qquad \mathbf{F} \equiv \mathbf{E} + \mathbf{N}^{(1)}. \tag{52}$$

In P85 a phase-independent flux $\mathbf{F}_s$ was derived for a zonally uniform basic flow (U) as $\mathbf{F}_s = \mathbf{F} + \mathbf{G}$, utilizing arbitrariness in adding any nondivergent vector to **F** in (52). In contrast, we (and TN97) derived a phase-independent flux based not only on the conservation of A but also on that of $\mathcal{E}$. Since $\mathbf{N}^{(1)} + \mathbf{N}^{(2)} = 0$ for unforced ($s' = 0$), stationary ($C_P = 0$) eddies, our flux is expressed as

$$\mathbf{W} = \frac{1}{2}(\mathbf{F} + \mathbf{H}^*) = \frac{1}{2}(\mathbf{E} + \mathbf{H}),$$

where $\mathbf{H}^* \equiv \mathbf{H} + \mathbf{N}^{(2)}$ as shown in (23). Since $\mathbf{F}_s = \mathbf{W}$ for a zonally uniform basic flow, it is readily obtained that $\mathbf{G} = (\mathbf{H}^* - \mathbf{F})/2$, which therefore represents a flux of a quantity $(\mathcal{E} - A)/2$ for stationary eddies. It should be noted that this quantity can be related to "pseudoenergy" (Andrews 1983; McIntyre and Shepherd 1987; Haynes 1988), which is expressed in our notations as $U(\mathcal{E} - A)$.

Generally, pseudoenergy obeys an exact (local) conservation law even for finite-amplitude disturbances on a zonally varying basic flow (McIntyre and Shepherd 1987; Haynes 1988). Conservation of pseudoenergy reflects the time invariance of a basic flow, whereas that of pseudomomentum reflects the translational invariance of a basic state in the zonal direction (e.g., Held 1987). Unlike pseudoenergy, an exact conservation of pseudomomentum for finite-amplitude perturbations is realized *only* for a zonally *uniform* basic flow. Hence, a conservation relation of pseudomomentum is necessarily an approximate one when extended to a zonally inhomogeneous basic state, as we needed to assume on several occasions during our derivation that the basic state is unforced and slowly varying in space, and that perturbations are small in amplitude as well. However, as P85 pointed out, pseudoenergy, if averaged over the wave phase, vanishes for any stationary waves even in the generalized Lagrangian-mean theory (Andrews and McIntyre 1978). For example, it is easily checked that $[\mathcal{E} - A]$ vanishes for stationary eddies in the form of a plane wave and so does $U[\mathcal{E} - A]$, where [ ] represents phase averaging. This is why **G** is nondivergent for stationary eddies under $s' = 0$. Furthermore, pseudoenergy depends strongly on the wave phase, as it consists only of the half-wavelength component in the almost plane-wave limit. Therefore, a pseudoenergy flux is not applicable to diagnosing phase-averaged statistics of stationary disturbances, and it may not be particularly convenient for visualizing a *snapshot* of the wave-packet propagation of migratory eddies.

Applying M and **W** to the simulated and observed atmospheric data, we have verified their phase-independency and ability to depict the wave-packet propagation of both stationary and migratory QG eddies. In particular, **W** is the first diagnostic tool capable of illustrating an *instantaneous* status of the *three-dimensional* propagation of a packet of migratory waves in a phase-independent manner. The price we ought to pay for it is that we need a priori knowledge of the local phase speed of the eddies, which should be either prescribed theoretically or estimated statistically in advance. It should be kept in mind that this estimation is apt to induce certain errors in the evaluation of **W**. For stationary eddies, we have shown that **W** can depict wave-packet propagation on a zonally varying basic flow in a more realistic manner than such a wave-activity flux as $\mathbf{F}_s$ defined for a zonally uniform basic flow, in a sense that **W** better represents the advective nature of $\mathbf{C}_g$. We have also shown that $\boldsymbol{\nabla}_H \cdot \mathbf{W}$ leads to a more realistic estimation of a wave source region than $\boldsymbol{\nabla}_H \cdot \mathbf{F}_s$. Of course, it may be enough to use $\mathbf{F}_s$ for diagnosing the planetary waves, although **W** applied to a zonally uniform basic flow is equivalent to $\mathbf{F}_s$. We claim that **W** is a useful diagnostic tool for disturbances embedded on a basic flow, which is asymmetric in the zonal direction in the presence of the planetary waves.

The validity of the approximations we used has also been assessed. In our applications, the residual term $\mathcal{R}$ is negligible almost everywhere, which means that the almost plane-wave assumption is reasonably valid. Yet,

Unauthenticated | Downloaded 08/23/22 02:00 PM UTC

our assessment indicates that the validity of the assumptions concerning a basic flow is more cautionary. Although qualitatively valid, those assumptions may result in nonnegligible errors in evaluating $\nabla \cdot \mathbf{W}$, especially when the QG scaling breaks down, for example, due to the tropopause intersection on a pressure surface, and/or when uncertainties in the estimation of C_P of migratory eddies are combined. Therefore $\mathbf{W}$ may not be particularly suited for the exact budget evaluation of M. Still, it is useful for illustrating (instantaneous) three-dimensional propagation of a wave packet, as we have demonstrated in several applications to stationary and migratory eddies in simulated and observed datasets. In addition, our flux has broader practical applicabilities than that of P85. Our conservation law just fits to the framework based on the separation between a three-dimensional time-mean flow and anomalies embedded on it. Therefore, our flux can readily be applied to such circulation anomalies defined as departures from a time-mean flow (e.g., the climatological-mean flow). In contrast, a certain ambiguity exists for Plumb's flux $\mathbf{F}_s$ for stationary eddies with respect to whether it is applied to eddies defined as total departures from an instantaneous zonally averaged flow or to the anomalies defined as above that are assumed to be embedded on a zonally averaged time-mean flow. In the former application, the flux field is dominated by the contribution of the planetary waves in the time-mean flow, which makes it difficult to isolate a rather small contribution from the anomalies. The latter application is unlikely to depict the wave-packet propagation associated with the anomalies as in a realistic manner as our flux can. Hence, our flux may be a useful tool for routine climate diagnoses in an operational center. In fact, our flux has been used in regular monthly climate diagnoses at the Japan Meteorological Agency since 2 yr ago, for analyzing stationary Rossby waves in pentad-mean anomaly fields as the departures from the climatological mean state.

Acknowledgments. Discussion with Dr. H. Sakuma of IGCR, the Frontier Research System for Global Change, was very helpful in clarifying our argument on the relationship between pseudomomentum and pseudoenergy. We thank Drs. Y. Matsuda, Y. Wakata, M. Takahashi, and Y.-Y. Hayashi of the University of Tokyo, Drs. Y. Kuroda, S. Maeda, and S. Takano of the Japan Meteorological Agency, and Dr. Yamamoto of Wakayama University for their constructive comments and suggestions. Dr. P. Kushner of the Princeton University and anonymous reviewers gave us critical comments, which also led to substantial improvement of our paper. Also, we thank Dr. T. Enomoto and Dr. M. Honda for providing us numerical data simulated in their latest works. This study is supported in part by the Grant-in-Aid for Scientific Research on Priority Areas (08241104) of the Japanese Ministry of Education, Science, Sports and Culture.

APPENDIX A

Derivation of Wave-Activity Conservation Law through "Local Coordinate Rotation"

An alternative approach to deriving an approximate conservation relation of wave-activity pseudomomentum M for a zonally varying basic flow is what may be called local coordinate rotation. We begin with a linearized PV equation on a zonally varying basic state as taken from (10):

$$\frac{\partial q'}{\partial t} - \frac{\partial \Psi}{\partial Y}\frac{\partial q'}{\partial X} + \frac{\partial Q}{\partial Y}\frac{\partial \psi'}{\partial X} = s'. \tag{A1}$$

We multiply (A1) by pq'/Q_Y and $p\psi'/(|\mathbf{U}| - C_P)$ to yield respective conservation relations of A and $\mathcal{E}$. Since X variations in Ψ and Q_Y are neglected under the assumption of a slowly varying basic flow, a derivation of a conservation relation of A can be somewhat simplified and becomes similar to that in P85. Likewise, a derivation of a conservation relation of $\mathcal{E}$ can also be somewhat simplified. We obtain an approximate conservation relation of M by combining those two relations:

$$\frac{\partial M}{\partial t} + \nabla_{(X,Y)} \cdot \mathbf{W}^{(X,Y)} = D', \tag{A2}$$

with

$$\mathbf{W}^{(X,Y)} = \frac{p}{2}\begin{pmatrix} (\psi_X'^2 - \psi'\psi_{XX}') + 2C_P M \\ \psi_X'\psi_Y' - \psi'\psi_{XY}' \\ \dfrac{f_0^2}{N^2}(\psi_X'\psi_z' - \psi'\psi_{Xz}') \end{pmatrix}. \tag{A3}$$

In (A2), $\nabla_{(X,Y)}$ is the three-dimensional divergent operator in the (X, Y, z) coordinate system. Finally, we manipulate (A3) rotating the local coordinate system back, in order to obtain an explicit expression of $\mathbf{W}$ on the latitude–longitude coordinate system.

APPENDIX B

Group Velocity of Rossby Waves on a Zonally Varying Basic Flow

Here, we derive an expression of the group velocity $\mathbf{C}_g$ of free Rossby waves on a zonally varying basic flow. We begin with an explicit form of the linearized PV equation (5) for free waves:

$$\frac{\partial q'}{\partial t} + U\frac{\partial q'}{\partial x} + V\frac{\partial q'}{\partial y} + \frac{\partial Q}{\partial x}u' + \frac{\partial Q}{\partial y}v' = 0. \tag{B1}$$

In the following, we assume that the buoyancy frequency N varies slowly in z and a vertical scale m^{-1} is much less than a constant scale height H. From (A1) with $s' = 0$, the phase speed C_P in the direction of the basic flow $\mathbf{U}$ is given by

Unauthenticated | Downloaded 08/23/22 02:00 PM UTC

$$C_P \approx |\mathbf{U}| - \frac{|\boldsymbol{\nabla}_H Q|}{|\mathbf{K}|^2}. \tag{B2}$$

Since $U/|\mathbf{U}| = Q_y/|\boldsymbol{\nabla}_H Q|$ and $V/|\mathbf{U}| = -Q_x/|\boldsymbol{\nabla}_H Q|$ for an unforced, ''pseudoeastward'' basic flow, we obtain from (B2)

$$U - \frac{Q_y}{|\mathbf{K}|^2} \approx \frac{U}{|\mathbf{U}|}C_P \quad \text{or} \tag{B3}$$

$$V + \frac{Q_x}{|\mathbf{K}|^2} \approx \frac{V}{|\mathbf{U}|}C_P. \tag{B4}$$

Based on (B1), the dispersion relation for a QG perturbation $\psi' = \psi_0 \exp(z/2H) \sin(kx + ly + mz - \omega t)$ may be represented as

$$\omega = k\left(U - \frac{Q_y}{|\mathbf{K}|^2}\right) + l\left(V + \frac{Q_x}{|\mathbf{K}|^2}\right). \tag{B5}$$

Then, with the aid of (B3) and (B4), the local group velocity is given by

$$\mathbf{C}_g = \begin{pmatrix} \omega_k \\ \omega_l \\ \omega_m \end{pmatrix} = \begin{Bmatrix} \dfrac{U}{|\mathbf{U}|}C_P + \left(\dfrac{2k^2Q_y}{|\mathbf{K}|^4}\right) - \left(\dfrac{2klQ_x}{|\mathbf{K}|^4}\right) \\ \dfrac{V}{|\mathbf{U}|}C_P + \left(\dfrac{2klQ_y}{|\mathbf{K}|^4}\right) - \left(\dfrac{2l^2Q_x}{|\mathbf{K}|^4}\right) \\ \dfrac{f_0^2}{N^2}\left[\left(\dfrac{2kmQ_y}{|\mathbf{K}|^4}\right) - \left(\dfrac{2lmQ_x}{|\mathbf{K}|^4}\right)\right] \end{Bmatrix}$$

$$= \mathbf{C}_U + \frac{2|\boldsymbol{\nabla}_H Q|}{|\mathbf{K}|^4|\mathbf{U}|}\begin{pmatrix} k^2U + klV \\ klU + l^2V \\ \dfrac{f_0^2}{N^2}(kmU + lmV) \end{pmatrix}. \tag{B6}$$

APPENDIX C

A Conservation Law of M and Its Flux W on the Pressure Coordinates

The PV equation on a β plane on the pressure (p) coordinates may be written as

$$\frac{\partial q}{\partial t} + u\frac{\partial q}{\partial x} + v\frac{\partial q}{\partial y} = s, \tag{C1}$$

where PV on the QG scaling is defined as

$$q = f_0 + \beta y + \frac{\partial^2 \psi}{\partial x^2} + \frac{\partial^2 \psi}{\partial y^2} + \frac{\partial}{\partial p}\left(\frac{f_0^2}{S^2}\frac{\partial \psi}{\partial p}\right). \tag{C2}$$

In (C2) a static stability parameter is defined by $S^2 = -\alpha(\partial \ln\theta/\partial p)$ where θ denotes potential temperature and α specific volume. Equation (C1) may be linearized as

$$\frac{\partial q'}{\partial t} + \mathbf{U}\cdot\boldsymbol{\nabla}_H q' + \mathbf{u}'\cdot\boldsymbol{\nabla}_H Q = s', \tag{C3}$$

and we obtain an approximate conservation relation of M after manipulations similar to those described in section 2.; that is,

$$\frac{\partial M}{\partial t} + \boldsymbol{\nabla}\cdot\mathbf{W} = D_T, \tag{C4}$$

with

$$\mathbf{W} = \frac{1}{2|\mathbf{U}|}\begin{pmatrix} U(\psi_x'^2 - \psi'\psi_{xx}') + V(\psi_x'\psi_y' - \psi'\psi_{xy}') \\ U(\psi_x'\psi_y' - \psi'\psi_{xy}') + V(\psi_y'^2 - \psi'\psi_{yy}') \\ \dfrac{f_0^2}{S^2}[U(\psi_x'\psi_p' - \psi'\psi_{xp}') + V(\psi_y'\psi_p' - \psi'\psi_{yp}')] \end{pmatrix} + \mathbf{C}_U M. \tag{C5}$$

Here, the wave-activity pseudomomentum is defined as $M = \frac{1}{2}(A + \mathcal{E})$ with $A = q'^2/(2|\boldsymbol{\nabla}_H Q|)$ and $\mathcal{E} = e/(|\mathbf{U}| - C_P)$.

REFERENCES

Andrews, D. G., 1983: A conservation law for small-amplitude quasi-geostrophic disturbances on a zonally asymmetric basic flow. *J. Atmos. Sci.,* **40,** 85–90.

——, 1984: On the existence of nonzonal flows satisfying sufficient conditions for instability. *Geophys. Astrophys. Fluid Dyn.,* **28,** 243–256.

——, and M. E. McIntyre, 1976: Planetary waves in horizontal and vertical shear: The generalized Eliassen–Palm relation and the mean zonal acceleration. *J. Atmos. Sci.,* **33,** 2031–2048.

——, and ——, 1978: On wave action and its relatives. *J. Fluid. Mech.,* **89,** 647–664.

——, J. R. Holton, and C. B. Leovy, 1987: *Middle Atmosphere Dynamics.* Academic Press, 489 pp.

Blackmon, M. L., J. M. Wallace, N.-C. Lau, and S. L. Mullen, 1977: An observational study of the Northern Hemisphere wintertime circulation. *J. Atmos. Sci.,* **34,** 1040–1053.

——, Y.-H. Lee, J. M. Wallace, and H.-H. Hsu, 1984: Time variation of 500-mb height fluctuations with long, intermediate and short time scales. *J. Atmos. Sci.,* **41,** 981–991.

Bretherton, F. P., and C. J. R. Garret, 1968: Wavetrains in inhomogeneous moving media. *Proc. Roy. Soc. London,* **A302,** 529–554.

Brunet, G., and P. H. Haynes, 1996: Low-latitude reflection of Rossby wave trains. *J. Atmos. Sci.,* **53,** 482–496.

Chang, E.-K. M., 1993: Downstream development of baroclinic waves as inferred from regression analysis. *J. Atmos. Sci.,* **50,** 2038–2053.

——, and I. Orlanski, 1993: On the dynamics of a storm track. *J. Atmos. Sci.,* **50,** 999–1015.

Edmon, H. J., B. J. Hoskins, and M. E. McIntyre, 1980: Eliassen–Palm cross sections for the troposphere. *J. Atmos. Sci.,* **37,** 2600–2616; Corrigendum, **38,** 1115.

Enomoto, T., and Y. Matsuda, 1999: Rossby wavepacket propagation in a zonally-varying basic flow. *Tellus,* **51A,** 588–602.

Haynes, P. H., 1988: Forced, dissipative generalizations of finite-amplitude wave-activity conservation relations for zonal and nonzonal basic flows. *J. Atmos. Sci.,* **45,** 2352–2363.

Held, I. M., 1987: New conservation laws for linear quasi-geostrophic waves in shear. *J. Atmos. Sci.,* **44,** 2349–2351.

Holton, J. R., 1992: *An Introduction to Dynamic Meteorology.* 3d ed. Academic Press, 511 pp.

Honda, M., K. Yamazaki, H. Nakamura, and K. Takeuchi, 1999: Dynamic and thermodynamic characteristics of atmospheric response to anomalous sea-ice extent in the Sea of Okhotsk. *J. Climate,* **12,** 3347–3358.

Unauthenticated | Downloaded 08/23/22 02:00 PM UTC

Hoskins, B. J., and D. J. Karoly, 1981: The steady linear response of a spherical atmosphere to thermal and orographic forcing. *J. Atmos. Sci.,* **38,** 1179–l196.

——, and T. Ambrizzi, 1993: Rossby wave propagation on a realistic longitudinally varying flow. *J. Atmos. Sci.,* **50,** 1661–1671.

——, I. N. James, and G. H. White, 1983: The shape, propagation and mean-flow interaction of large-scale weather systems. *J. Atmos. Sci.,* **40,** 1595–1612.

Karoly, D. J., R. A. Plumb, and M. Ting, 1989: Examples of the horizontal propagation of quasi-stationary waves. *J. Atmos. Sci.,* **46,** 2802–2811.

Kuroda, Y., 1996: Quasi-geostrophic 3-dimensional E–P flux of stationary waves on a sphere. *J. Meteor. Soc. Japan.,* **74,** 563–569.

McIntyre, M. E., 1982: How well do we understand the dynamics of stratospheric warmings? *J. Meteor. Soc. Japan,* **60,** 37–65.

——, and T. G. Shepherd, 1987: An exact local conservation theorem for finite-amplitude disturbances to non-parallel shear flows, with remarks on Hamiltonian structure and on Arnold's stability theorems. *J. Fluid Mech.,* **181,** 527–565.

Nakamura, H., 1994: Rotational evolution of potential vorticity associated with a strong blocking flow configuration over Europe. *Geophys. Res. Lett.,* **21,** 2003–2006.

——, M. Nakamura, and J. L. Anderson, 1997: The role of high- and low-frequency dynamics in the blocking formation. *Mon. Wea. Rev.,* **125,** 2074–2093.

Naoe, H., Y. Matsuda, and H. Nakamura, 1997: Rossby wave propagation in idealized and realistic zonally varying flows. *J. Meteor. Soc. Japan,* **75,** 687–700.

Plumb, R. A., 1985: On the three-dimensional propagation of stationary waves. *J. Atmos. Sci.,* **42,** 217–229.

——, 1986: Three-dimensional propagation of transient quasi-geostrophic eddies and its relationship with the eddy forcing of the time-mean flow. *J. Atmos. Sci.,* **43,** 1657–1678.

Simmons, A. J., J. M. Wallace, and G. W. Branstator, 1983: Barotropic wave propagation and instability, and atmospheric teleconnection patterns. *J. Atmos. Sci.,* **40,** 1363–1392.

Takaya, K., and H. Nakamura, 1997: A formulation of a wave-activity flux for stationary Rossby waves on a zonally varying basic flow. *Geophys. Res. Lett.,* **24,** 2985–2988.

Trenberth, K. E., 1986: An assessment of the impact of transient eddies on the zonal flow during a blocking episode using localized Eliassen–Palm flux diagnostics. *J. Atmos. Sci.,* **43,** 2070–2087.

Uryu, M., 1974: Mean zonal flows induced by a vertically propagating Rossby wave packet. *J. Meteor. Soc. Japan.,* **52,** 481–490.

Vanneste, J., and T. Shepherd, 1998: On the group-velocity property for wave-activity conservation laws. *J. Atmos. Sci.,* **55,** 1063–1068.

Wallace, J. M., G. H. Lim, and M. L. Blackmon, 1988: Relationship between cyclone tracks, anticyclone tracks, and baroclinic waveguides. *J. Atmos. Sci.,* **45,** 439–462.

Unauthenticated | Downloaded 08/23/22 02:00 PM UTC